Stability Criteria of Reversible Pump Turbines

Rakel Ellingsen

NTNU

Norwegian University
of Science and Technology

Department of Energy
and Process Engineering

EPT-M-2014-29

MASTER THESIS

for

Student Rakel Ellingsen
Spring 2014

Stability criteria of Reversible Pump turbines

Stabiliteskriterer for reversible pumpeturbiner

Background and objective

In reversible pump turbines stabile operation in both pump and turbine mode of operation is essential. There is certain criteria connected to the characteristics of the machine, as well as to the head loss of the system that has to be fulfilled. In addition, for a system with surge shafts, the Thoma instability is also an issue.

The candidate has, through her project work, identified the criteria connected to the characteristics in pumping mode of operation and performed simulations to illustrate the stability problem. In her Master, the candidate shall verify the theory by means of experiments at a pump test rig at TU Berlin.

The objective is to verify the stability criteria for a centrifugal pump.

The following tasks are to be considered:

1 Gather information and develop a simulation model for the actual test rig at TU Berlin
2 Plan the instrumentation and data acquisition system
3 Measure the pump characteristics
4 Set the pump and system in a predicted unstable operation and measure the oscillations
5 Analyse and conclude

Within 14 days of receiving the written text on the master thesis, the candidate shall submit a research plan for his project to the department.

When the thesis is evaluated, emphasis is put on processing of the results, and that they are presented in tabular and/or graphic form in a clear manner, and that they are analyzed carefully.

The thesis should be formulated as a research report with summary both in English and Norwegian, conclusion, literature references, table of contents etc. During the preparation of the text, the candidate should make an effort to produce a well-structured and easily readable report. In order to ease the evaluation of the thesis, it is important that the cross-references are correct. In the making of the report, strong emphasis should be placed on both a thorough discussion of the results and an orderly presentation.

The candidate is requested to initiate and keep close contact with his/her academic supervisor(s) throughout the working period. The candidate must follow the rules and regulations of NTNU as well as passive directions given by the Department of Energy and Process Engineering.
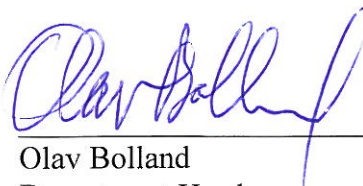
Risk assessment of the candidate's work shall be carried out according to the department's procedures. The risk assessment must be documented and included as part of the final report. Events related to the candidate's work adversely affecting the health, safety or security, must be documented and included as part of the final report. If the documentation on risk assessment represents a large number of pages, the full version is to be submitted electronically to the supervisor and an excerpt is included in the report.

Pursuant to "Regulations concerning the supplementary provisions to the technology study program/Master of Science" at NTNU §20, the Department reserves the permission to utilize all the results and data for teaching and research purposes as well as in future publications.

The final report is to be submitted digitally in DAIM. An executive summary of the thesis including title, student's name, supervisor's name, year, department name, and NTNU's logo and name, shall be submitted to the department as a separate pdf file. Based on an agreement with the supervisor, the final report and other material and documents may be given to the supervisor in digital format.

☒ Work to be done in lab (Water power lab, Fluids engineering lab, Thermal engineering lab)
☐ Field work

Department of Energy and Process Engineering, 14. January 2014

Olav Bolland
Department Head

Torbjørn K. Nielsen
Academic Supervisor

Research Advisor: Pål Tore Storli

Acknowledgement

ii

Abstract

The objective in this Master's Thesis was to verify the stability criteria for a centrifugal pump. Operation of an unstable pump may lead to either exponential or oscillatory unstable behaviour of both pressure and volume flow of the water in the conduit system. This is of course unwanted, and fulfilling the stability criteria is desirable.

The idea is to test an unstable pump, which was done at the Technical University Berlin (TU) in Germany. Most of the test set-up was already installed, but a new pump and a pressure accumulator was inserted. Unfortunately the experiment was not able to verify the stability criteria systematically, because the set-up was a closed loop without reservoirs; and because the different parameters affecting the stability were difficult to change.

The experiment was educational even though the stability criteria were not verified. Different tasks were executed at TU, like installing the pressure accumulator and a pressure sensor, and measuring the pump characteristic. The work with the Master's Thesis also improved the candidate's understanding of the stability criteria and the dynamic behaviour of the water in general.

A simulation program was made in Matlab, and the aim of the program was to simulate the oscillations of the water in the conduit system. Most of the parameters put into Matlab were measured at TU, except the volume of the air inside the pressure accumulator. This volume affects the frequency of the oscillations a lot, but a good estimation of the volume of the air, made the simulations quite similar to the measured results. In addition to simulating the existing set-up, the simulation program made it easy to vary the parameters affecting the stability criteria. The simulation program was tested this way, and the stability criteria seem to be correct.

Samandrag

Målet med denne masteroppgåva var å verifisere stabilitetskriteria for ei sentrifugalpumpe. Køyring av ei ustabil pumpe kan føre til ei ustabil eksponentiell eller oscillatorisk endring i trykk og volumstraum for vatnet i rørsystemet. Dette er sjølvsagt uønska, så oppfylling av stabilitetskriteria er derfor viktig.

Ideen er å teste ei ustabil pumpe, og dette vart gjort ved Technical University Berlin (TU). Bortsett frå ei ny pumpe og ein trykkakkumulator, var mesteparten av testriggen allereie installert. Forsøket var dessverre ikkje i stand til å systematisk verifisere stabilitetskriteria, og dette var fordi testriggen var ei lukka sløyfe utan magasin, og fordi dei ulike parametrane som påverkar stabiliteten var vanskeleg å endre.

Eksperimentet var lærerikt, sjølv om stabilitetskriteria ikkje vart bekrefta. Fleire ulike oppgåver vart utført, som å installere trykkakkumulatoren og ein trykksensor, og å måle pumpekarakteristikkar. Arbeidet med masteroppgåva auka også kandidatens forståing av stabilitetskriteria, og den dynamiske oppførselen til vatnet generelt.

Eit simuleringsprogram, som vart laga i Matlab, hadde som formål å simulere svingingane av vassmassane i rørsystemet rundt pumpa. Dei fleste av parametrane som Matlab trenger for å rekne på desse svingingane vart målt ved TU, men det gjaldt ikkje volumet av lufta inne i trykkakkumulatoren. Dette volumet har stor påverknad på frekvensen av dei svingande vassmassane, men ei god estimering av volumet av lufta gjorde simuleringane ganske like dei målte resultata. I tillegg til å simulere testriggen, gjorde simuleringsprogrammet det lett å variere dei ulike parametrane som påverka stabilitetskriteria. Simuleringsprogrammet vart testa på denne måten, og stabilitetskriteria verkar til å vere korrekt.

Contents

List of Figures

List of Tables

Nomenclature

Symbol	Description	Unit
A	Area	m^2
a	Speed of sound	m/s
a	Constant in the pump characteristic	-
A_s	Surge shaft area	m^2
b	Constant in the pump characteristic	-
c	Constant in the pump characteristic	-
C	Elastic compliance	$m^4 s^2/kg$
f	Friction factor	-
f	Frequency	Hz
g	Acceleration of gravity	m/s^2
H	Head	m
$H0$	Constant in the pump characteristic	-
k	Loss coefficient	s/m^2
L	Length	m
n	Rotational speed	rpm
P	Power	W
p	Pressure	Pa
Q	Volumetric flow rate	m^3/s
Q^*	Constant in the pump characteristic	-
t	Time	s
V	Volume	m^3
z	Number of pole pairs motor	-
z	Number of blades	-
z	Surge shaft level	m

Greek letters

Symbol	Description	Unit
β	Relative flow angle	^{0}
Δ	Small time quantity	-
κ	Heat capacity ratio	-
ρ	Water density	kg/m^3

Sub- and superscripts

Symbol	Description
0	Initial point at steady state
1	Downstream the surge shaft
2	Upstream the surge shaft
a	Air inside pressure accumulator
acc	Pressure Accumulator
eq	Equivalent, for the equivalent area
f	Friction
gv	Guide vanes
$loss$	Losses
m	Minor losses
n	Time Step
np	Net pump
nt	Net turbine
p	Pump
rb	Runner blades
rot	Rotational
s	Shaft
s	System
st	Static
th	Thoma
V	Valve
wh	Water Hammer

Abbreviation

Symbol	Description
CFD	Computational Fluid Dynamics
dec	Decreasing
inc	Increasing
$NTNU$	Norwegian University of Science and Technology
RMS	Root Mean Square
rpm	Revolutions per minute
RPT	Reversible Pump Turbines
TU	Technical University in Berlin

Chapter 1

Introduction

Reversible pump turbines (RPT) are popular today because they make it much easier to adjust the production of electricity to the demand. Many new renewable energy sources have a limited period in which production is possible, like solar panels only produce electricity when the sun is up. Hydro power plants with reservoirs can adjust their production much closer to the demand. A pump turbine adds even more regulation since it can be driven as a pump on a sunny day when the production from the solar panels is greater than the demand in the market. When the sun goes down, the pump turbine will be switched to generating mode in order to satisfy the demand for electricity.

A RPT is a compromise between a good pump and a good turbine, and this may lead to unstable behaviour both in pump- and turbine mode of operation. The runner of a pump turbine is similar to a centrifugal pump, as will be explained in chapter 3.1. Centrifugal pumps on the other hand usually do not experience problems with this unstable behaviour, because they easily can be constructed stable. The stability of centrifugal pumps was studied, and to a certain extent solved in the late 70s and early 80s. Many of the literature sources used in this Master's Thesis are therefore quite old. The results the researchers found then is still valid. Even though the stability of a centrifugal pump usually is not a problem, the knowledge is useful for pump mode of a RPT.

This Master's Thesis will look at how the water in the conduit system is affected by the design of the RPT in pump mode. The stability criteria found in the candidate's Project Thesis will be tested. This will be done in an experiment at a pump laboratory at the Technical University Berlin (TU). A centrifugal pump, which is unstable for some volume flows, will be used. The focus is not on the design itself, but on the dynamic of the water in the pipes. Unstable operation in pump mode may lead to oscillations that increase in amplitude. This is of course an undesired behaviour.

Before arrival in Berlin, a literature study will be carried out. A simulation program will also be adjusted so it hopefully predicts the results from TU.

Chapter 2

Background

2.1   Previous work

Greitzer already published an article called "The stability of pumping systems" [5] in 1981. In this article several pumping systems are studied and the stability criterion for each system is discussed. One of these pumping systems was a simple pump set-up quite similar to the set-up in this Master. Greitzer also defines static stability and dynamic stability, as explained in chapter 3.4.

Many of the available centrifugal pump books also have some information about pump stability [3] [7] [8] [9]. Chapter 3.4 cover some of the results from these books. Many of these books, as well as the article written by Greitzer, are relatively old. This reveals that pump stability is not a new subject, and it also reveals that some of the issues with pump stability were solved in the 80s.

In the article "First-Order Pump Surge Behavior" by Rothe and Runstadler from 1978, an experiment on an unstable centrifugal pump was carried out [10]. The available theory at that time could reasonable predict the results from the experiments!

Today's research on pump stability is more concerned with what happens inside the pump, and especially the use of Computational Fluid Dynamics (CFD) makes this possible. These types of investigations make it possible to study the flow phenomena, which are the reason for the instabilities, and a short introduction is given in chapter 3.2.1. This Master's Thesis will on the other hand be more concerned with the stability criteria investigated on the 70s and 80s.

A hypothesis of a stability criteria for a RPT in pump mode was established in the candidate's project thesis during the fall of 2013 [25]. This was done by looking at the differential equations' eigenvalues in the conduit system. The equations are given in chapter 3.3. The result from this project and from the literature is tested on a centrifugal pump in this Master.

2.2 Test facility

The Waterpower Laboratory at the Norwegian University for Science and Technology (NTNU) has one RPT, which is designed by Grunde Olimstad. He did his PhD at the Waterpower Laboratory in 2012, and the topic of the thesis was stability in turbine mode of a RPT. The RPT at NTNU is unstable in turbine mode, since Olimstad wanted to test the stability criteria in turbine mode. Unfortunately this RPT is stable for all operating points in pump mode. Since the goal of this Master is to test an unstable pump, this RPT cannot be used in this Master. A different RPT or centrifugal pump was necessary, resulting in testing a centrifugal pump at the TU.

Chapter 3

Theory

3.1   Reversible Pump Turbines

A reversible pump turbine (RPT) needs to work well in both turbine mode and pump mode of operation. Good design of the RPT is therefore important, and it is today possible to create a RPT with a cycle efficiency of 70-80 % [11].

Several types of pump turbines are available, but the Francis type RPT is commonly used, and will be in focus in this chapter. First some of the design criteria for the RPT will be discussed.

3.1.1   Design criteria

The distance between the upper reservoir and the lower reservoir is called H_{st}. This is the static head and is showed in figure 3.1.
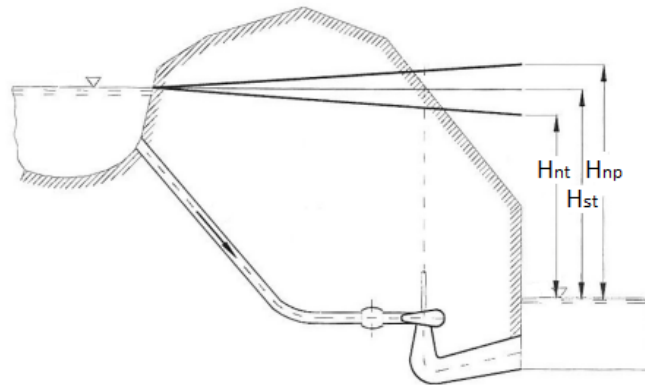
Figure 3.1: Visualisation of the difference in available head in turbine mode and demanded head in pump mode of a RPT [1].

In turbine mode, the hydraulic losses is subtracted from the static head. The available head H_{nt} is therefore less than H_{st}. In pump mode the delivered head H_{np} must overcome both the static head and the hydraulic losses, and H_{np} is consequently bigger than H_{st}. In order to work well in pump mode, the RPT must be designed according to H_{np}.

The lifting head of a RPT strongly depends on the outer diameter of the pump. This means that the outer diameter of a RPT needs to be bigger than the outer diameter for a Francis turbine, as illustrated in figure 3.2 [2]. If the diameter is too small, the RPT will not be able to lift the water to the upper reservoir.
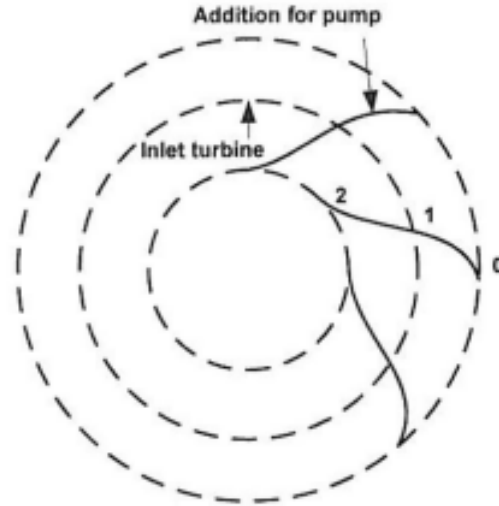
Figure 3.2: The difference in outer diameter for a RPT and a Francis turbine [2]

In figure 3.2 the addition in diameter for a RPT is demonstrated. 0 is the inlet of the RPT (in turbine mode) and 1 refers to the inlet for a Francis turbine. 2 refers to the outlet.

3.1.2 Physical structure of a RPT

A pump turbine has spiral casing, guide vanes, stay vanes and draft tube just like a Francis turbine.

A Francis runner and a centrifugal pump impeller have quite different angles of the blades. A RPT is a compromise between a good pump and a good turbine, but the design of the runner/impeller will be more or less like a centrifugal pump impeller [1] [8]. This is done both to be able to lift the water and to increase the stability of the RPT in pump mode. Flow separation, recirculation and losses pose a bigger problem in pump mode because of the decelerated flow [12]. This is another reason for why the runner's/impeller's design is similar to the centrifugal pump. The curvature of the blades and the blade leaning is then adjusted to make the runner as good as possible in turbine mode of operation [1].

The guide vanes turn out to be beneficial for pump operation [13]. One of the advantages is that the efficiency with guide vanes are higher than without when the RPT is operated off-design [13]. The guide vanes also make it easier to adjust the flow rate through the RPT, making it easier to accomplish stable operation.

3.2   The centrifugal pump

This sub chapter will focus on those parts of the centrifugal pump theory, which is necessary to know in order to understand the stability criteria in chapter 3.4. Both the pump- and system characteristics will be presented here, since they are important for the stability. The system dynamics is also important for stability, and this will be covered in chapter 3.3.

3.2.1   The pump characteristic

In pump mode the pressure rise over the pump is usually presented in a H-Q diagram, where H is the head [m] and Q is the volume flow [m^3/s]. A curve called the pump characteristic depict how the delivered head from the pump varies with volume flow. This curve is connected to the design of the pump, and its shape is impossible to change without changing the pump design. Ideally the slope of this curve should be negative because this implies stable operation, as is further explained in chapter 3.4. This is the case for most centrifugal pumps, but in this Master's Thesis an unstable pump characteristic is essential.
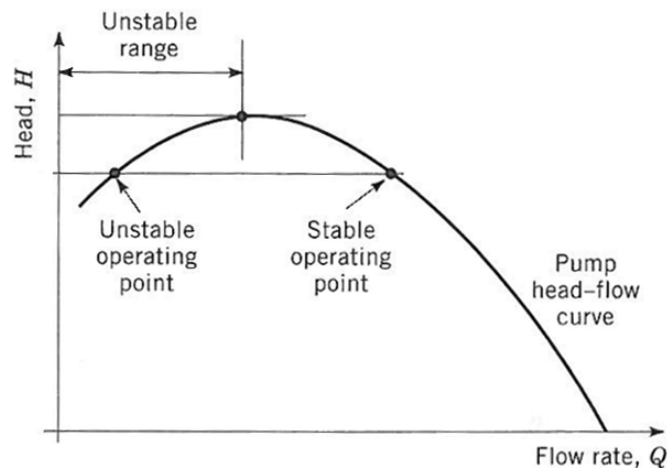
Figure 3.3: Illustration of unstable and stable regions of the pump characteristic [3].

In figure 3.3 an example of an unstable pump characteristic is illustrated. The pump characteristic is unstable when the slope is positive for some volume flows, which is the case for the left region of the pump characteristic in figure 3.3.

The most important parameter affecting the pump characteristic is the relative flow angle β. β smaller than 90° leads to a negative slope of the pump characteristic, while a β that exceeds 90° leads to a positive slope of the pump characteristic [1]. For more information on how to estimate the pump characteristic, see chapter 2 in [14].

The pump characteristic is usually more unstable for small volume flows, possibly due to the channels not being filled as much as intended. The best efficiency operating point is usually far away from this unstable region at part load, so unstable behaviour is usually

not a problem [15]. RPTs do sometimes operate on part load, and it is then important to have stable operation for all volume flows.

Chapter 2 mentioned that today's research on instabilities in pumps are mostly concerned with what happens inside the pump, and how this affects the pump characteristic. Pumps may experience problems with both separation of flow, rotating stall and other flow related instabilities, which impact the pump characteristic due to losses. Several CFD simulations and experiments have been made in attempt to figure out these mechanisms.

Rotating stall is cells of flow separation, which emerge at different locations in the impeller [16]. The phenomena occur when the pump operates with too high incident angles [17]. This leads to unstable behaviour of the water inside the pump, and it is one of the main reasons for unstable pump operation [18], because the losses lead to a drop in the pump characteristic [8]. The rotating stall leads to pressure fluctuations, stated by the article "Experimental study of the Pressure Fluctuations in a Pump Turbine at large partial flow conditions" to be 20 % of the rotational frequency of the impeller/runner [18]. The frequency of the rotating stall may also vary from around 0.1 to 0.8 of the rotation frequency [18].

Centrifugal pumps do usually not have guide vanes. This makes it harder to regulate their capacity, but it is possible by either changing the speed of rotation of the pump or the losses in the system. The rotational speed has an effect on the pump characteristic, see figure 3.4: The higher the speed of rotation n the higher H.
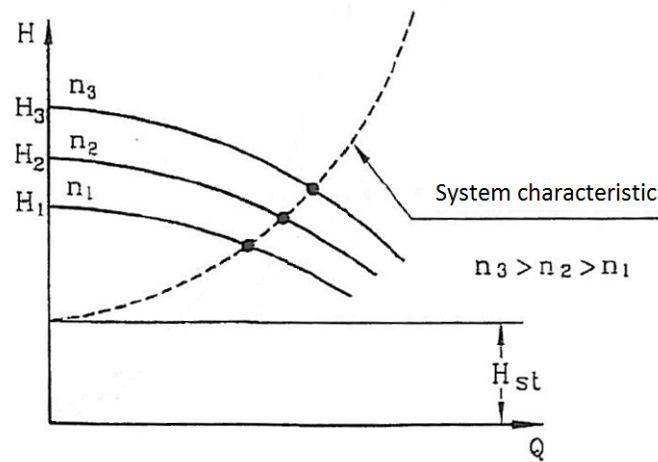
Figure 3.4: Change in operational point due to a change in the speed of rotation, n [4].

3.2.2 The system characteristic

The system around the pump needs a certain head H_s, and the system characteristic gives this head as a function of, Q. Both the static head H_{st} and the losses are of great importance, since the pump must overcome both these factors in order to lift the water from the lower to the upper reservoir. The system characteristic, H_s, can usually be written like equation 3.1 [19].

$$H_s = H_{st} + H_{loss} = H_{st} + Q^2(k_f + k_m) \tag{3.1}$$

Subscript f is here friction losses and m is the minor losses, which are losses in bends, valves etc. k is a factor, which can be both constant and a variable. Equation 3.1 reveals that the system characteristic often has a parabola shape. The bigger the k_f and k_m coefficients are, the steeper the system characteristic will be. At $Q = 0$ m^3/s the system demands the static head H_{st}.

In pump mode, the pump needs to deliver the same head as demanded by the system. The operational point is therefore where the pump- and system characteristic intersect. This is showed in figure 3.5, where the pump characteristic is the red line and the system characteristic is the blue line.
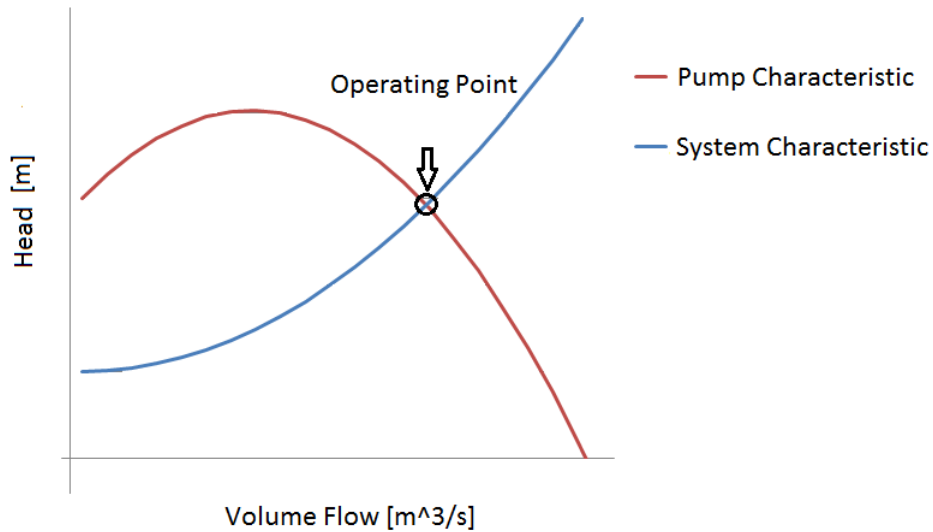
Figure 3.5: An example of a pump characteristic and a system characteristic.

The easiest way to regulate the volume flow for a centrifugal pump is to vary the losses in the system. This will change the system characteristic, because Q and k_m in equation 3.1 will change. Closing a throttle valve ensures this, thereby increasing k_m and the slope of the system characteristic steepens, see figure 3.6.
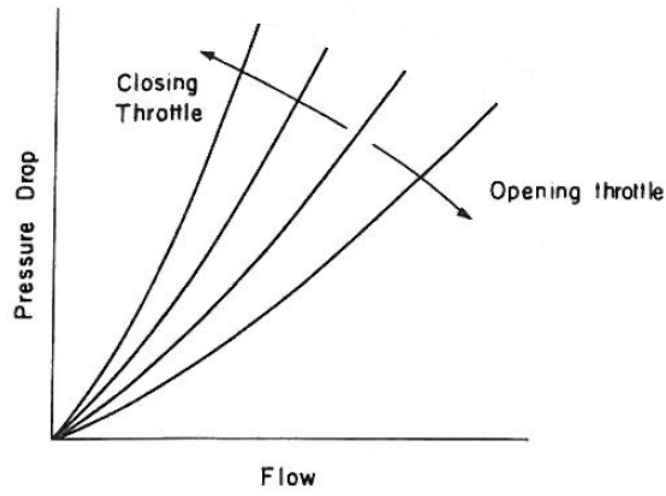
Figure 3.6: Change in slope of system characteristic due to change in opening degree of throttle valve [5]

3.3 System dynamics and U-tube oscillations

The design of the conduit system is of great importance for the kind of instabilities studied in this Master.

It is normal to insert a surge shaft in a pumped storage power plant, when the distance between the upper reservoir and the RPT is long, see figure 3.7. Consequently the pressure rise in front of the turbine after a sudden closure of the valve reduces. This big increase in pressure is due to elasticity of the water, and it is called the water hammer effect [20]. The surge shaft will on the other hand create a new problem: u-tube oscillations, where the water masses oscillate between the free surfaces [20].
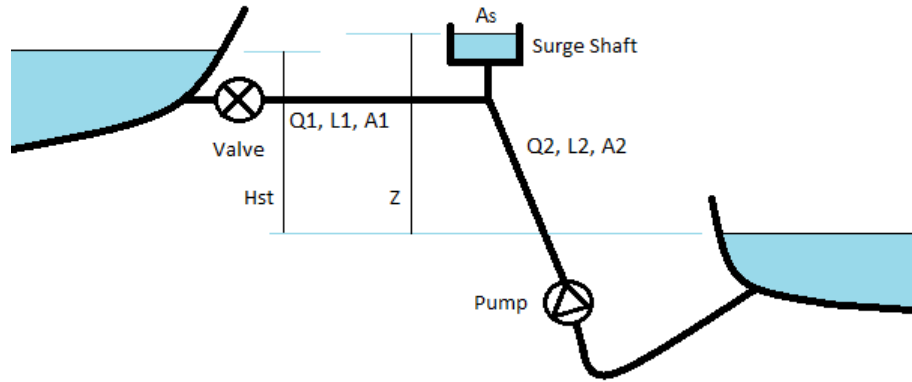
Figure 3.7: An example of a pumped storage power plant with surge shaft.

Equations 3.2, 3.3 and 3.4 show how the volume flows, and the water level in the surge shaft in figure 3.7, changes over time when the water is assumed to be incompressible.

$$\frac{dQ_1}{dt} = \frac{gA_1}{L_1}(z - Hst - k_1 Q_1^2) \tag{3.2}$$

$$\frac{dQ_2}{dt} = \frac{gA_2}{L_2}(Hp - z - k_2 Q_2^2) \tag{3.3}$$

$$\frac{dz}{dt} = \frac{1}{As}(Q_2 - Q_1) \tag{3.4}$$

k is here sum of the friction and the minor losses according to equation 3.1. A is here the cross-sectional area of the pipe/tunnel, L is the length and g is the acceleration of gravity. The subscript 1 is means downstream the surge shaft, while subscript 2 means upstream the surge shaft. H_p is the pressure delivered by the pump, and it is given by the pump characteristic and Q.

A small change in volume flow from the pump ,Q_2, will lead to a pressure increase in the pipe. This leads to a difference between Q_2 and the volume flow in front of the valve, Q_1, which increases the level of the surge shaft z. If the surge shaft area, A_s is small, z becomes big fast. The pressure in front of the valve increases as well, and the valve will respond with more volume flow. When Q_1 is bigger than Q_2, z will decrease.

11

Thoma was the first to derive an expression for the smallest surge shaft area that leads to stable operation for a turbine A_{th}, see equation 3.5. The derivation is given in [20].

$$A_s \geq A_{th} = \frac{LA}{2gf(H_{st} - z)} \qquad (3.5)$$

f is here a friction factor.

A. Anderson wrote an article called "Surge Shaft Stability with Pumped-Storage Schemes" in 1984. He looked at the Thoma area and tried to find a more complex and correct formula, which also takes into account the junction losses to the surge shaft, different layouts of the surge shaft and the pump mode of a RPT [15]. Different shapes of surge shafts will give different junction losses according to Anderson, and this loss increases the stability and decreases A_{th} for a turbine [15].

Some Norwegian hydro power plants use an air cushion instead of a surge shaft, where the air cushion consists of trapped pressurized air. The biggest advantage of such an air cushion is that the distance between the pump and its cushion can be smaller than if substituting it with a surge shaft. This will decrease the time it takes for the pressure waves to travel, which again will decrease the pressure rise. For the air cushion the spring in the system is non-linear and stiffer [20].

The air in the accumulator is assumed to be an ideal gas, and the compression process is assumed to be both adiabatic and reversible. The air thus behaves according to equation 3.6, enabling an equivalent area, A_{eq}, to be calculated, see equation 3.7. This area can roughly be used as the surge shaft area in equation 3.5 [20].

$$H_{acc}V^{\kappa} = H_{acc,0}V_0^{\kappa} \qquad (3.6)$$

$$A_{eq} = (\frac{1}{A_{acc}} + \frac{H_{p0}\kappa}{V_0})^{-1} \qquad (3.7)$$

V is here the volume of the air, κ is the heat capacity ratio and the subscript acc means accumulator.

The frequency of the u-tube oscillations depend on the system around the pump or turbine. Equation 3.8 shows how to calculate the frequency of the u-tube oscillations with an air cushion [20]. For a surge shaft, A_s is used instead of A_{eq} in equation 3.8.

$$f_{u-tube} = \sqrt{\frac{g}{A_{eq}\frac{L}{A}}}\frac{1}{2\pi} \qquad (3.8)$$

3.4 Stability

Stability is a word used in many contexts, so making a short explanation to the word's meaning in this Master is necessary.

This chapter explains stability in pump mode, but first a more general view on stability is given.

3.4.1 Stability in general

A basic idea when it comes to stability, is to look at what happens if a system experiences a small perturbation. If the system manages to come back to it's starting point, the system is stable [5].

Greitzer [5] divided the stability in static and dynamic stability. In the static case no oscillations occur after a small perturbation, while for the dynamic case oscillations will occur. Both types are seen in figure 3.8.

(a) Statically Stable   (b) Statically Unstable

(c) Dynamically Stable   (d) Dynamically Unstable
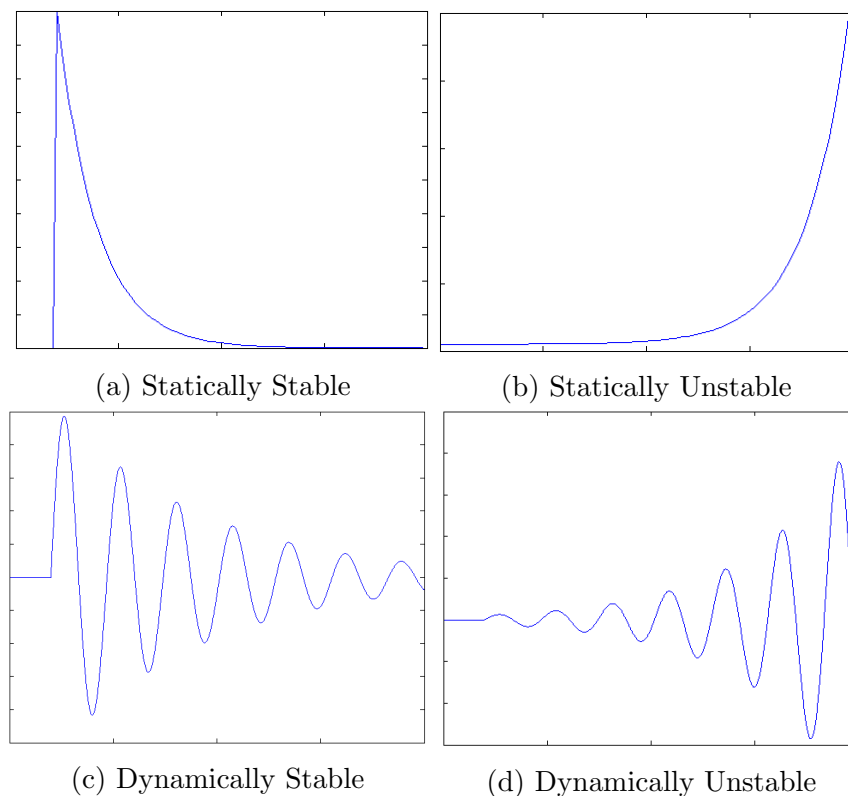
Figure 3.8: Illustration of static and dynamic stability and instability with time on the x-axis and a variable on the y-axis

Figure 3.8a represents the statically stable system. A small disturbance will not lead to permanent change, and after a small time period the system is back where it started, without any oscillations. Figure 3.8b shows no sign of oscillations, but the small disturbance leads to an exponential growth. This system is then statically unstable. Figures 3.8c and 3.8d are the dynamically stable and the dynamically unstable situation respectively.

13

Chapter 3.2 states the slope of the pump characteristic to be the most important parameter when it comes to stability of pumping systems. When the slope of the pump characteristic is negative for all volume flows, no instabilities occur [7] [8]. For the static stability criterion, only the pump and system characteristics are studied, and this is further explained in sub chapters 3.4.2 and 3.4.3.

Greitzer found that the system can experience instabilities even though the static criteria is fulfilled [5], because the dynamic stability criterion is less stringent than the static stability criteria. Dynamic instability, or surging, is recognized by large amplitude oscillations of the water. This is seldom for pumps, but more common for compressors, because of the need for compressibility in the system [21].

Self-exited vibrations are essential for dynamic instability, meaning that oscillations increase because energy is put into the system. Such vibrations require the system to be able to store and give back energy during the vibration cycle [7]. It is also necessary to have a possibility for free oscillations and a source of impulses that will trigger the oscillations [9]. For a pump the triggering of the unstable oscillations is the unstable pump characteristic [9], which is further explained with the help of figure 3.9. The spring in the system is the compressed air in the pressure accumulator, and the water can oscillate between free surfaces [9].
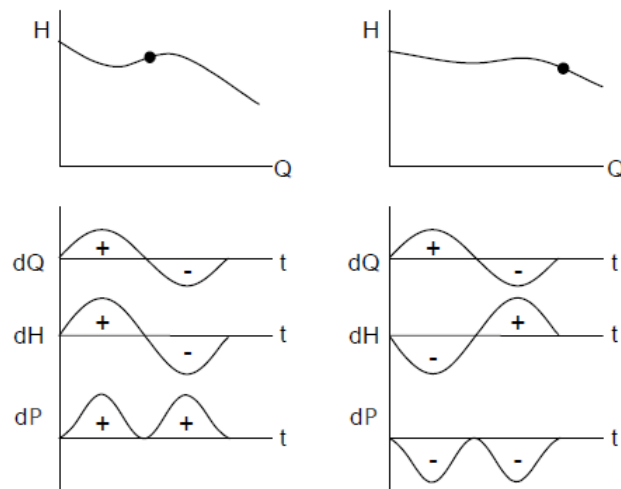
Figure 3.9: Illustration of dynamic stability and instability [5].

In the left part of figure 3.9, the operational point is in the unstable region of the pump characteristic. Here the problem is that Q and H oscillate in phase. Thus the power P is positive, since $P = \rho g Q H$, meaning that there is a net energy input to the water during the cycle [22]. The amplitude of the oscillations continues to increase until the energy input equals the dissipation in the system [21]. The oscillations will then have a constant amplitude, called a limit cycle [21]. Usually this surge period is under 2 seconds, corresponding to a frequency around 0.5 Hz [21].

However the operational point to the right in figure 3.9 is in the stable region of the pump characteristic. H and Q is then in opposite phases and P is then negative,indicating a net energy dissipation caused by damping of the oscillations [5].

Both Anderson [6] and Greitzer [5] derived the static- and dynamic stability criteria for a simple system with discrete inertia and elasticity. Anderson concluded with two different systems that will give rise to two different stability criteria, and they are presented here. Both systems consist of a pump, a pressure accumulator or surge shaft, and a rigid-column duct. The system where the accumulator is next to the valve, as seen in sub chapter 3.4.2 is studied first. The criteria explained in this sub chapter, are the most common ones from the literature, and this sub chapter is thus easier to rely on. For the case explained in sub chapter 3.4.3, the accumulator is placed next to the pump, and the stability criteria are here opposite to the ones in sub chapter 3.4.2.

The systems in figures 3.10 and 3.11 are very simplistic. Losses in the junction between the pressure accumulator and the main pipe, is for example not included. Such losses are assumed to make the system more stable, since they will dampen the oscillations.

The placement of the valve is important, and if it's placed too close to the outlet of the pump, no instabilities occur [9]. In addition, the frictional losses in the system need to be small compared to the losses through the valve for unstable behaviour [9]. For the criteria in sub chapters 3.4.2 and 3.4.3, a valve characteristic is introduced, and the slope of this characteristic is assumed to be given only by the valve, and not by other losses in the system. The slope of this valve characteristic is given by equation 3.1 for zero friction, and the slope is thus smaller then for the system characteristic.

3.4.2   The accumulator next to the valve
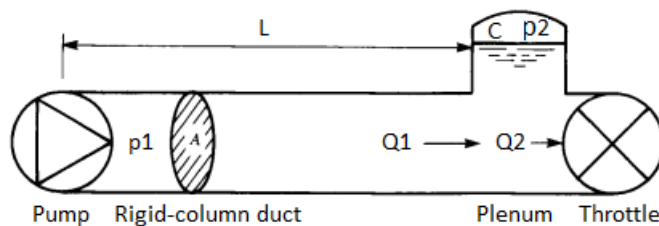
Figure 3.10: The accumulator close to the valve [6].

The rate of change of Q_1 is given in equation 3.9, while equation 3.10 gives the rate of change of pressure p_2.

$$\frac{dQ_1}{dt} = \frac{A}{L\rho}(p_1 - p_2) \tag{3.9}$$

$$\frac{dp_2}{dt} = \frac{1}{C}(Q_1 - Q_2) \tag{3.10}$$

C is here the elastic compliance in the system, where equation 3.11 gives C for an accu-

mulator, and equation 3.12 gives C for a surge shaft [6].

$$C_{acc} = \frac{V_a}{p_{acc}\kappa} \tag{3.11}$$

$$C_s = \frac{A_s}{g\rho} \tag{3.12}$$

The valve in figure 3.10 is affected by a change in pressure, and it is then important that any change in pressure in the valve is bigger than any change in the pump, which leads to the static stability criterion seen in equation 3.13. This criterion is also found in Greitzer [5].

$$\frac{dH_v}{dQ} > \frac{dH_p}{dQ} \tag{3.13}$$

dH_v/dQ and dH_p/dQ are here the slopes of the valve and pump characteristic respectively.

When the criterion in equation 3.13 is fulfilled, a small increase in for example Q, will lead to a small increase in H_p, which is given by the pump characteristic. If dH_v/dQ is larger then dH_p/dQ, the needed pressure increase in the valve is higher than the increased H_p. The pump can thus not deliver enough head to the system, and Q will decrease back to its initial value.

If the criterion in equation 3.13 is not fulfilled, the increased Q leads to the pump delivering more head than needed, and Q will continue to increase!

A too small dH_p/dQ is not good for stability either, as seen in equation 3.14.

$$\frac{Ag}{L}\frac{dH_p}{dQ} > \frac{1}{C}\frac{1}{\rho g}\frac{dQ}{dH_v} \tag{3.14}$$

For a small dH_p/dQ, a small change in operational point makes the volume flow from the pump change a lot compared to the change in head. This leads to a slow acceleration of Q_2, if the term A/L is small as well, as seen in equation 3.9. A big elastic compliance makes the increase in p_2 small, according to equation 3.10, which is negative for the valve. The slope of the system characteristic also matters, and a big dH_v/dQ means the pump corresponds quickly to an increase in pressure, which is good for stability.

3.4.3 The accumulator next to the pump

Anderson also looked at the system in figure 3.11, where the accumulator is close to the pump.
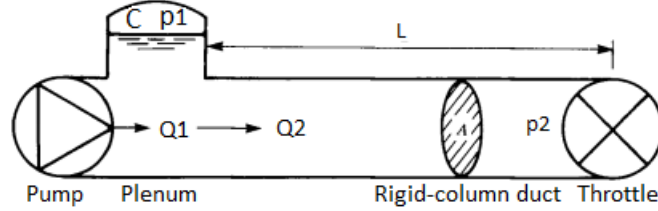
Figure 3.11: The accumulator close to the pump [6].

The rate of change of p_1 is given in equation 3.15, while equation 3.16 gives the rate of change of Q_2.

$$\frac{dp_1}{dt} = \frac{1}{C}(Q_1 - Q_2) \tag{3.15}$$

$$\frac{dQ_2}{dt} = \frac{A}{L\rho}(p_1 - p_2) \tag{3.16}$$

In figure 3.11, it's a change in Q_2 which affects the valve. It is therefore important that dQ/dH_v is larger than dQ/dH_p, because this means the valve dampens any changes in volume flow from the pump. This criteria can be written as in equation 3.17 or as in equation 3.18.

$$\frac{dQ}{dH_v} > \frac{dQ}{dH_p} \tag{3.17}$$

$$\frac{dH_p}{dQ} > \frac{dH_v}{dQ} \tag{3.18}$$

A too large dH_p/dQ, is not good for stability either, because the pressure in the system can then increase. This leads to the criterion seen in equation 3.19.

$$\frac{Ag}{L}\frac{dH_p}{dQ} < \frac{1}{C}\frac{1}{\rho g}\frac{dQ}{dH_v} \tag{3.19}$$

For the system in figure 3.11, a large dH_p/dQ, means a change in operational point in the pump leads to a large increase in delivered pressure, and a small increase in delivered volume flow. This impacts p_1, according to equation 3.15, because the accumulator responds to a change in volume flow. A large elastic compliance means a small increase in p_1, which again will mean a small increase in Q_2 according to equation 3.16. The valve does then not see the changes in pressure from the pump, and if dH_v/dQ is too large, the valve will not manage to reduce the pressure in the system.

17

3.5 Vibrations

In addition to the u-tube oscillations, different rotor-stator interactions may occur. One such vibration is the interaction between the impeller or runner and the guide vanes.

Equation 3.20 shows how the speed of rotation, n, is connected to the number of pole pairs z and the frequency f.

$$n = \frac{60f}{z} \tag{3.20}$$

The rotational frequency of the pump is the frequency fed to the motor f, divided by the motor's number of pole pairs, see equation 3.21.

$$f_{rot} = \frac{n}{60} = \frac{f}{z} \tag{3.21}$$

The runner blade frequency, f_{rb}, is calculated with the help of equation 3.22. This frequency may occur every time a runner blade passes the non-rotating parts.

$$f_{rb} = f_{rot} z_{rb} \tag{3.22}$$

z_{rb} is here the number of runner/impeller blades.

The guide vane frequency, f_{gv}, can be calculated with equation 3.23.

$$f_{gv} = f_{rot} z_{gv} \tag{3.23}$$

z_{gv} is here the number of guide vanes.

Chapter 3.3 mentioned the water hammer effect. An estimation of the pressure waves' frequency, f_{wh}, is achieved with equation 3.24.

$$f_{wh} = \frac{a}{4L} \tag{3.24}$$

a is here the speed of sound of water and L the length the pressure waves must travel.

Chapter 4

Method

4.1 What I want to test

The goal of this Master is to verify the stability criteria from chapter 3.4 through experiments on a centrifugal pump with an unstable pump characteristic.

According to the hypothesis for the static stability criterion in chapter 3.4.2, the slope of the system characteristic needs to be relatively flat for instabilities to occur. By varying the losses in the system with a throttle valve, the slope of the system characteristic can be changed. The static head is important also, and ideally the static head should be adjustable. For low static head, the system characteristic is very steep for small volume flows, and the static stability criterion is always fulfilled. The static stability criterion for the system seen in equation 3.17 is on the other hand very difficult to fulfil.

It is not necessarily easy to reach the unstable region of the pump characteristic and at the same time have an almost flat system characteristic. Closing of the valve while the pump operates in the stable region, moves the operational point to the left. If the valve is closed enough the pump may enter the unstable region, but the slope of the system characteristic is then quite steep. Both a reduced speed of rotation or an increased static head may force the operational point to move to the left.

If the power input from the pump is bigger than the dissipative forces during the oscillation cycle, the system is dynamically unstable. This may lead to oscillations of the water with increasing amplitude. The pressure accumulator in the set-up must be able to handle these oscillations. Ideally it should be possible to vary the pressure and the volume of the accumulator, in order to test the stability criteria given in equations 3.14 and 3.19. The slope of both the pump-and system characteristics also matters, and being able to vary the static head, the speed of rotation and the losses are important for both the static and the dynamic stability criteria.

4.2 The laboratory set-up

Most of the set-up of the laboratory was already installed at TU. The only changes done was to insert an unstable pump and to build and insert the pressure accumulator. The pump was already installed at arrival in Berlin, while the accumulator was connected to the pipe after arrival. Chapters 4.2.2 and 4.2.3 elaborate on the pump and the pressure accumulator respectively.

Figure 4.1 shows the set-up of the experimental test rig.
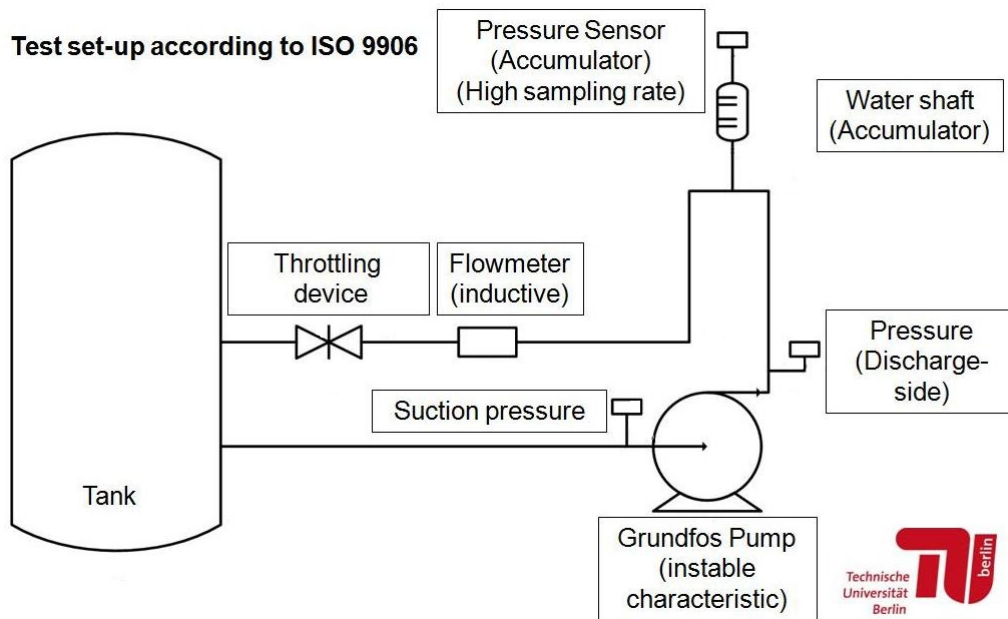
Figure 4.1: The set-up of the laboratory test rig at TU, Berlin

Table 4.1 shows some of the dimensions in figure 4.1. A is the cross sectional area in square meter and L is the length in meter. Acc is short for accumulator, while no sub script means the pipes around the pump.

Constant	Value
A_{acc}	0.0201
L_{acc}	0.6
A	0.091
L_1	8
L_2	2

Table 4.1: The dimensions of the pipes and the accumulator in the laboratory set-up.

The idea is to measure the pump characteristic with the help of one pressure sensor upstream and one pressure sensor downstream the pump. The volume flow is also important. By measuring the pressure increase over the pump at different volume flows, the pump

characteristic can be plotted.

The pump set-up was built after the ISO9906 standard called "Rotodynamic Pumps - Hydraulic performance acceptance test - Grades 1, 2 and 3" [23]. According to the standard, the length of the pipes should be long, so the inlet of the pipe is uniform and not influenced by bends for example. The standard also restrict the maximum temperature of the water and other parameters. The temperature of the water should not exceed 40°C during testing of pumps according to the standard. Change in density is the main reason for this, which influence the efficiency. This Master's Thesis does not focus on the performance or efficiency tests, and some of the aspects in the standard is therefore not very important here.

4.2.1   Motor

The motor driving the pump has two pairs of poles, and a nominal speed of rotation of 1480 revolutions per minute (rpm). It is designed for 50 Hz, but in this experiment it is run from 25 Hz to 45 Hz. The speed of rotation (in rpm and Hz) for each frequency can be calculated with equations 3.20 and 3.21, and the result is seen in table 4.2.

Frequency to motor f [Hz]	Speed of rotation n [rpm]	Speed of rotation f_{rot} [Hz]
25	750	12.5
30	900	15.0
35	1050	17.5
40	1200	20.0
45	1350	22.5

Table 4.2: The speed of rotation for the different frequencies.

4.2.2   The pump and casing

The pump used in this experiment is a pump from Grundfos, which was found at the storage room at TU. It is known to have an unstable pump characteristic, and the impeller has six blades. Figure 4.2 shows a picture of a pump equal to the one installed in the set-up. The casing has no blades.

Figure 4.2: The centrifugal pump used in the laboratory set-up in Berlin

4.2.3 The pressure accumulator

(a) A picture of the pressure accumulator
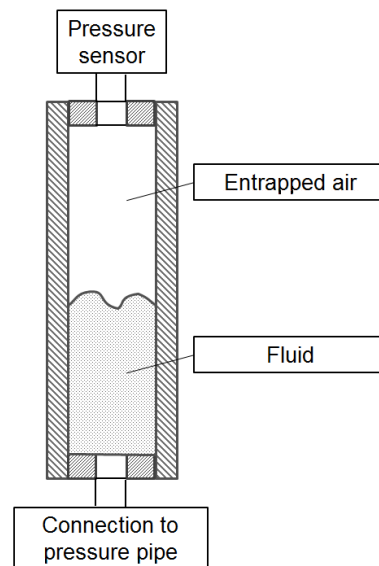
(b) A drawing of the pressure accumulator

Figure 4.3: The pressure accumulator

The pressure accumulator, seen in figure 4.3, is made at TU. Air is trapped inside the accumulator, like in figure 4.3b and the pressure of this air depends on the head delivered by the pump as well as the pressure in the big tank. It is made by a see-through plastic pipe so oscillations in water level might be possible to see.

The water level inside the accumulator is adjusted, thus visible inside the accumulator before the pump is started. If the level is too low, a valve can be opened at the top of the accumulator, releasing some air causing the pressure to go down. The valve is then closed when the level is visible. If on the other hand the level is very high before even

starting the pump, it might be necessary to lower the level by lowering the level in the big tank. This is done by letting some of the water inside the tank out.

The pressure sensor at the top is measuring the pressure of the trapped air with 100 samples per second. A higher sampling rate would give even more data assumable without necessity. The signal from the sensor goes to a computer, where it is processed through LabVIEW. Unfortunately there was no time to learn LabVIEW in the short amount of time spent in Berlin. The programming of the newly installed pressure sensor was therefore done by someone who already knew LabVIEW. Both the flow meter and the pressure sensors for the suction and discharge side of the pump was already installed and connected to the computer and to LabVIEW.

Between the main pipe and the accumulator, the junction is very narrow, and the losses are therefore assumed to be quite big.

The results from the pressure accumulator were analysed with the help of the Matlab function psd. This Fourier transform the results, so it is possible to find, which frequency is the dominant one for the different measurements. In order for the Fourier transform to work, the input signals must have a periodic behaviour. Both the method and a very similar source code to the one used in this Master's Thesis are found in [24].

4.3 The test procedure

The frequency converter is started while the valve is open. It takes only a couple of seconds before the pump reaches the speed corresponding to the chosen frequency of the frequency converter. The volume flow through the pump is then at its biggest for the given frequency, and the first operational point is recorded here. The handle of the valve is then turned, reducing the volume flow. This shifts the operational point to the left. A flow meter is installed close to the handle of the valve, so it is easy to see how the flow changes while you turn. The flow meter gives Q in m³/h, and this is the unit used for the rest of this Master's Thesis.

The distance between the chosen measurements varies with both volume flow and frequency. The idea is to take more measurements in the unstable region of the pump characteristic than in the stable region. For the stable region the operational point was typically saved for every 100 m³/h. When the slope of the characteristic flattens out, or becomes positive (for smaller volume flows), every 50 m³/h was saved. Table 4.3 presents which operational points are saved for each frequency.

The pump characteristic was measured for different frequencies. Both the pump and the motor is designed for 50 Hz, but this was not accomplished because the cable between the frequency converter and the motor would be too warm at 50 Hz. The measured frequencies were 25, 30, 35, 40 and 45 Hz.

For all frequencies the valve was first closed and then opened again, meaning that for all frequencies there are two sets of measurements. This was done mostly to see if hys-

Operational Point	Frequency [Hz]				
[m³/h]	25	30	35	40	45
0	X	X	X	X	X
50	X	X	X	X	X
100	X	X	X	X	X
150	X	X	X	X	X
200	X	X	X	X	X
250	X	X	X	X	X
300	X	X	X	X	X
350	X	X	X	X	X
400	X	X	X	X	X
450			X	X	
500	X	X	X	X	X
550			X	X	
600	X	X	X	X	
650					X
700		X	X	X	
750					
800			X	X	
850					X
900				X	
950					X

Table 4.3: The measurements done for different volume flows and different frequencies. X means that a measurement is done.

teresis was present. It is also a big advantage to have more than one set of measurements. In addition, the measurement of the pump characteristic was done twice for some of the frequencies. This was done mostly because the pressure sensor on top of the pressure accumulator fell off during the first series of measurements.

The temperature limit of 40 °C mentioned in chapter 4.2, was surpassed in these experiments. This is easily accomplished after running the pump for a while, because the set-up is a closed loop, and the pump adds energy to the system. Hopefully this did not impact the results. The pipes and the pump are designed to handle even higher temperatures, explaining why the high temperatures did not damage any of the equipment. The maximum temperature during the experiment was 41.8 °C at 45 Hz. This was the last measurement, and the temperature was already above 40 °C before start up. The 45 Hz frequency was therefore done quite fast to keep the temperature as low as possible.

I was at TU for only one week, and calibration of the different sensors used in the experiment was therefore not conducted. Other tasks were done instead, like helping with the installation and building of the pressure accumulator and pressure sensor, and participating in an exercise for students at TU at the pump rig. Necessary training was also done. In the two last days, many experiments were executed and I did most of the work alone.

4.4   The simulation program

The simulation program used in this Master's Thesis, is a continuation of the simulation program made in the candidate's Project's Thesis in the fall of 2013 [25]. It has been adjusted during the Master's thesis to simulate the laboratory set-up in Berlin. The source code to the simulation program is found in appendix B, and a detailed description of the program is found as comments in this code.

To solve the basic differential equations for the volume flows and the pressure in the accumulator, seen in chapter 3.3, Euler's method is utilized. In the project thesis a surge shaft was included, while in the laboratory in Berlin a pressure accumulator is used.

The results of the equations are plotted over time, and it is then possible to compare the result to the plots in figure 3.8, to see if the system is stable or not. Each time the script is run, different plots are made showing how both the pressure in the accumulator, the volume flow and the power change with respect to time. The program calculates the frequency of the oscillations in the accumulator pressure, and this can be compared to the frequency of the Fourier transformed results from the pressure accumulator in Berlin.

The length and the cross-sectional area of pipes and accumulator used in the program are the same as in Berlin, see table 4.1. The pump characteristics in the program were also adjusted to the measured characteristics in Berlin, with the help of equation A.1 and the variables a, b, c, H0 and Q*. They were adjusted for each frequency, so they fitted the curve as good as possible, and are seen in table A.1 in appendix A.

The volume of the air inside the pressure accumulator was not measured in Berlin. This was unfortunate, because the size of the air volume affects the mass oscillations, and it is important in the equations solved in Matlab. The solution was to use a volume coefficient and multiply this with the dimensions of the accumulator. The coefficient should be between 0 and 1, where 1 means that the accumulator is filled with air. 0 means that the accumulator is filled with water.

An Excel sheet was created with all the information needed in the Matlab script. When the script runs, it reads information from Excel. It will also write information to the same Excel sheet after the end of the simulation. The simulation program also calculates the slope of the pump- and system characteristics in a chosen operational point.

The slope of the system characteristic can be varied, for a given operational point, by including a static head. The bigger the static head, the bigger the opening of the valve needs to be in order for the system characteristic and the pump characteristic to intersect in the chosen operational point. For a big H_{st}, the slope of the system characteristic becomes smaller. Including a static head in the simulation program, makes it therefore possible to see how the slope of the system characteristic impacts the stability.

Chapter 5

Results

This chapter highlights the most important results from the measurements done at TU and from the simulation program. The results from TU consist of both the head increase over the pump and volume flow, which combined give the pump characteristic, and the results from the pressure accumulator. The simulation program plotted different sorts of plots, but the power oscillations have been chosen here.

First the pump characteristic for the different f is presented. Chapter 5.2 presents the Fourier transformed results from the pressure accumulator, for both unstable and stable regions of the pump characteristic. The last sub chapter shows some of the results from the simulation program.

5.1 The pump characteristic

All the measurements of the pump head, H_p and the volume flow are combined in figure 5.1. All the frequencies f are run both up and down, and some of them are also done twice, as mentioned in chapter 4.3. Table 4.3, also from chapter 4.3, shows an overview of which operational points are measured for different frequencies.
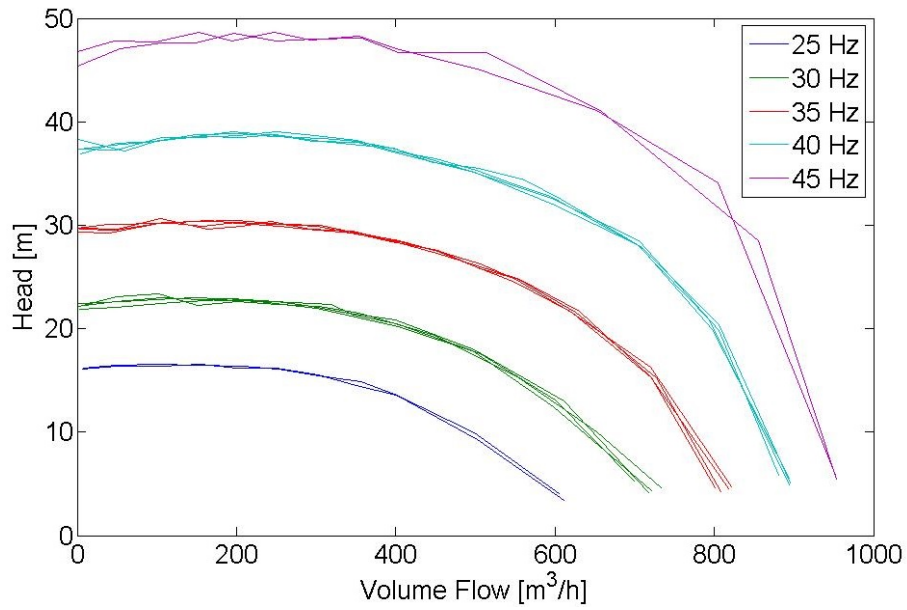
Figure 5.1: All the different measurements of the pump characteristic for all the frequencies.

In figure 5.2 the average of the measurements in figure 5.1 is calculated.
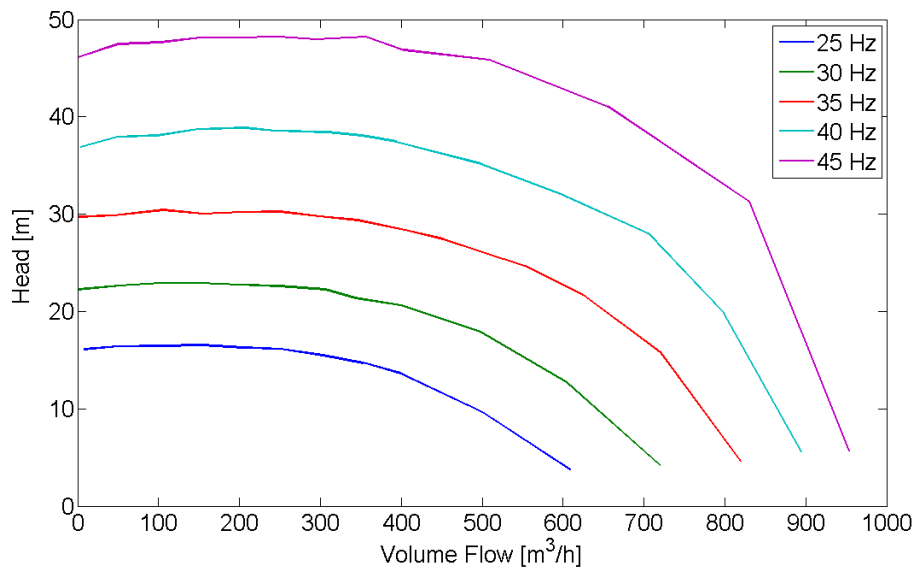
Figure 5.2: The pump characteristics for different frequencies: average of all measurements.

5.2 Results from the pressure accumulator

The results from the pressure accumulator were Fourier transformed and plotted, with amplitude (from Root Mean Square (RMS)) on the y-axis and frequency on the x-axis. This chapter presents some of these plots. Two operating points in the unstable characteristic ($Q = 50$ m^3/h and $Q = 100$ m^3/h) are studied first. Secondly, one operating point in the stable region of the pump characteristic is presented ($Q = 500$ m^3/h), before a short summary at the end of this sub chapter.

5.2.1 Unstable region of the pump characteristic

Both the operational points where $Q = 50$ m^3/h and $Q = 100$ m^3/h is in the unstable region of the pump characteristic, according to figure 5.1. By looking at both these operational points, it should be possible to see, which frequencies vary with volume flow and which frequencies are constant for the two operational points.

Figure 5.3 presents the results for $Q = 50$ m^3/h, and figure 5.4 for $Q = 100$ m^3/h.
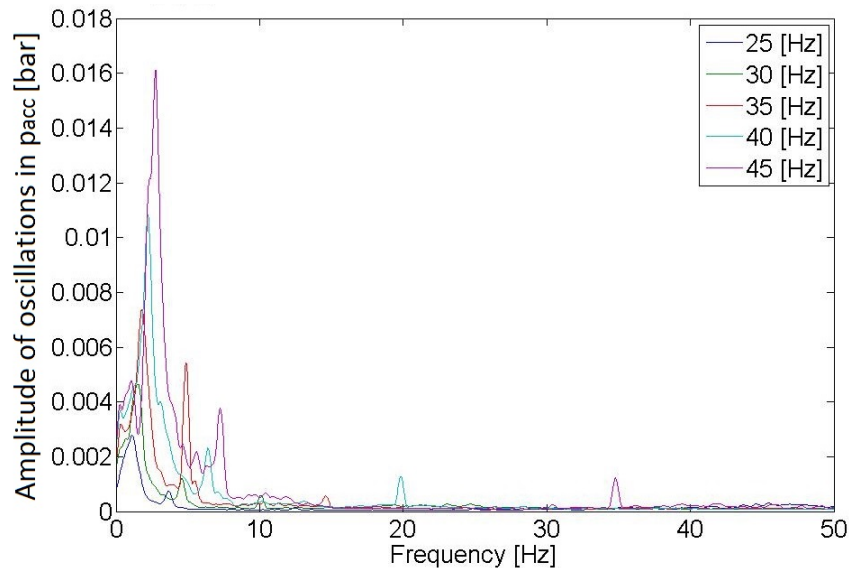
Figure 5.3: The result after the Fourier transform for all frequencies for Q=50 m^3/h.
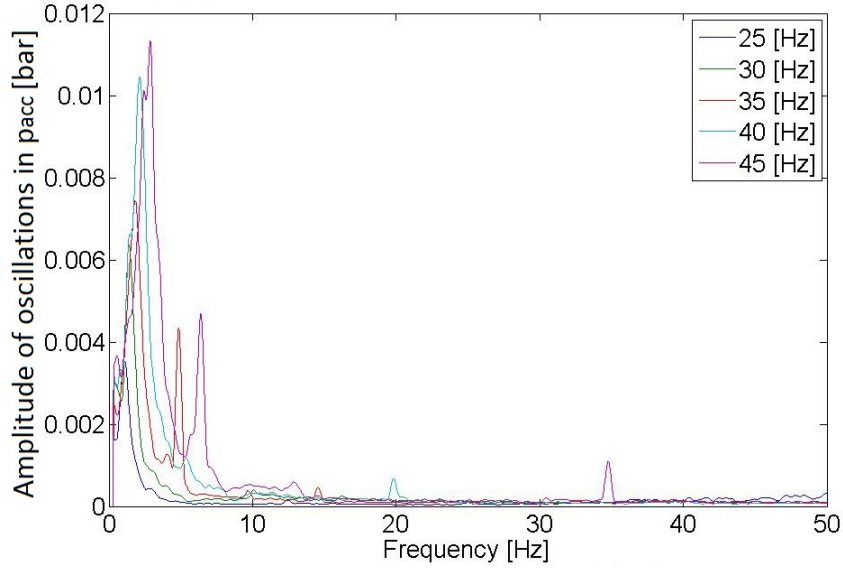
Figure 5.4: The result after the Fourier transform for all frequencies for $Q=100$ m^3/h.

There are two quite high peaks between 1 Hz and 8 Hz in figures 5.3 and 5.4.

The peak around 20 Hz, for the 40 Hz curve in figures 5.3 and 5.4, fits the speed of rotation of the pump seen in equation 4.2. There are two pole pairs in the motor, which makes this frequency 20 Hz, according to equation 3.21. It is also possible to see a small peak around 12.5 Hz for the 25 Hz curve.

The peak around 35 Hz in figures 5.3 and 5.4, may be connected to the water hammer effect. By using $L = 10.5$ m and $a = 1450$ m/s, the water hammer freqeuncy is 34.5 Hz, according to equation 3.24.

In figures 5.3 and 5.4 it is not that easy to see the different frequencies. The operational point where $Q = 100$ m^3/h, and $f = 35$ Hz, is therefore presented in figure 5.5.

30
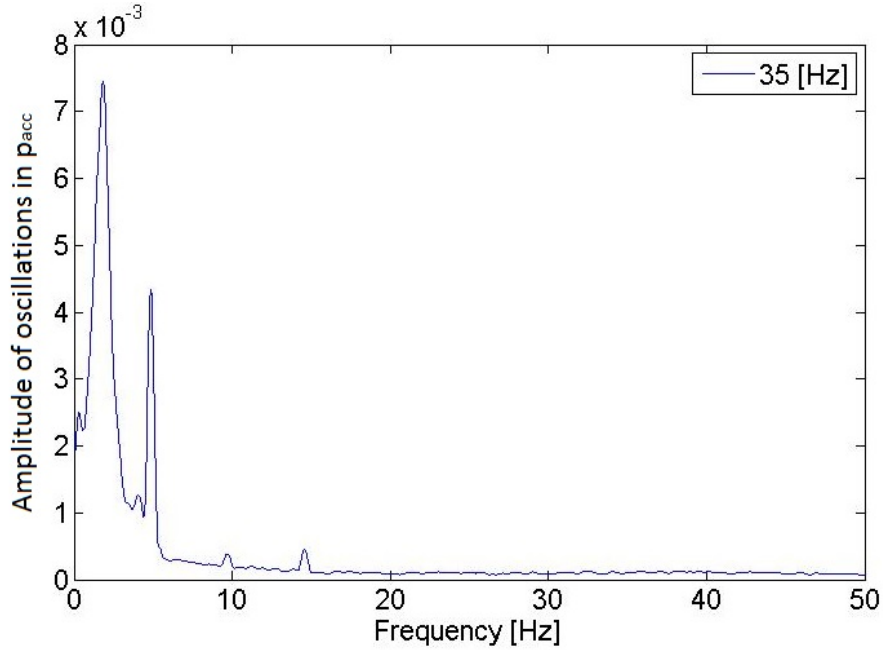
Figure 5.5: The results from the Fourier transform for $f = 35$ Hz and $Q = 100$ m^3/h.

Figure 5.5 shows the results after the Fourier transform for f=35 Hz and $Q = 100$ m^3/h. The frequency and amplitude value of the four peaks are represented in table 5.1.

Root Mean Square	Frequency [Hz]
0.00542	1.824
0.00230	4.859
0.00035	9.718
0.00049	14.58

Table 5.1: The peaks in figure 5.5

Please notice that 2·4.859=9.718 and 3·4.859=14.58. It is therefore assumed that peak number three and peak number four are connected to peak number two.

Both figures 5.3 and 5.4 were for the case where the volume flow was decreasing. The analysis for the decreasing flow was also executed for some of the measuring series. Figure 5.6 presents the result for $Q = 100$ m^3/h and $f = 45$ Hz for both increasing and decreasing volume flow.

Many of the other operational points were tested to see if increasing or decreasing Q might effect the outcome of the Fourier transform. In general, the result is that they are quite similar. With $Q = 500$ m^3/h the results are different though, as seen in the next sub chapter.
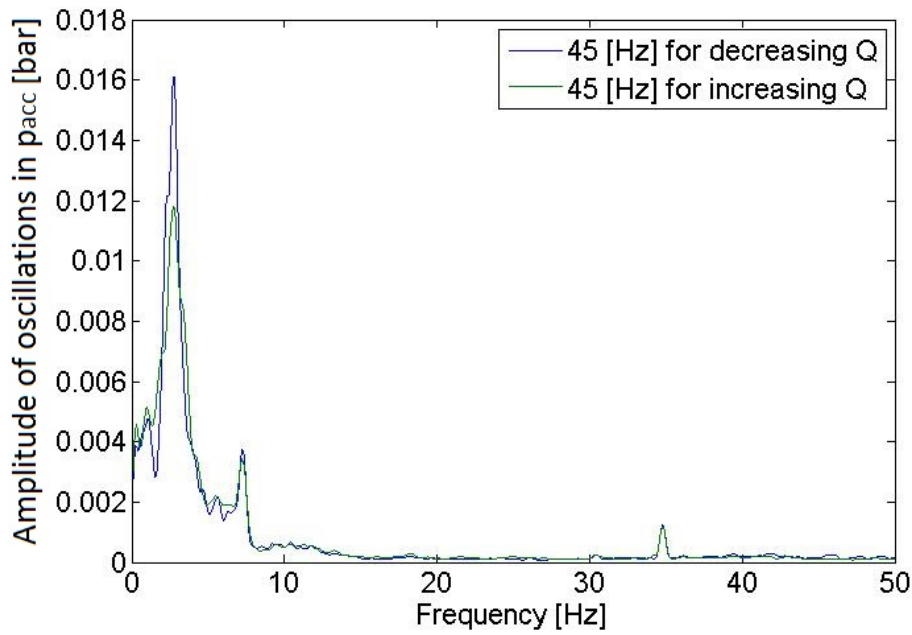
Figure 5.6: The result after the Fourier transform for 45 Hz for $Q = 50$ m^3/h for both increasing and decreasing volume flow.

5.2.2   Stable region of the pump characteristic

The operational point where $Q = 500$ m^3/h is in the stable region of the pump characteristic, according to figure 5.2. Figure 5.7 shows the results for $Q = 500$ m^3/h.
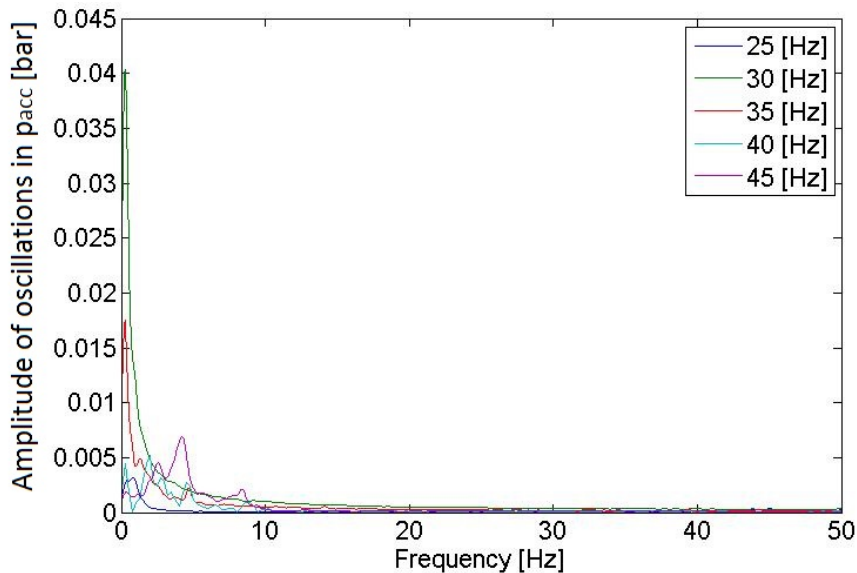
Figure 5.7: The results from the Fourier transform for $Q = 500$ m^3/h for the decreasing volume flows.

Figure 5.7 shows very different results than figures 5.3 and 5.4. The peak around 0.25 Hz in figure 5.7 is for example very big, and the idea to take the result from another

measurement then presented itself. The result in figure 5.7 is from the measurement where the valve is closing, which means that the volume flow is decreased. Figure 5.8 shows the result for the measurement, where Q is increased at the operational point of $Q = 500$ m^3/h.
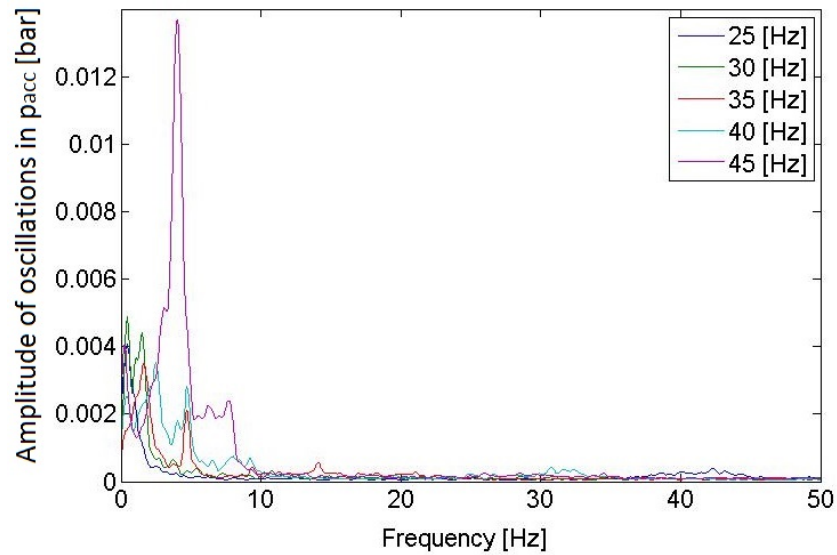
Figure 5.8: The results from the Fourier transform for $Q = 500$ m^3/h for the increasing volume flows.

Figure 5.8 shows the measurement where Q is increasing. The strange peak around 0.25 Hz in figure 5.7 is not present in figure 5.8. The rest of the result is not that different from figure 5.7. It is therefore assumed that the peak around 0.25 Hz in figure 5.7 is noise and therefore wrong.

Figure 5.9 presents the 45 Hz curve from both figures 5.7 and 5.8.
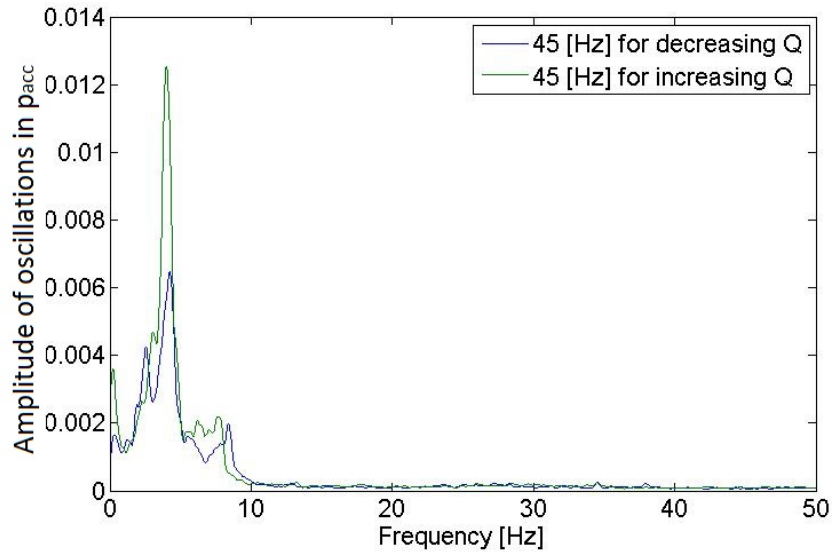
Figure 5.9: The result after the Fourier transform for 45 Hz for Q=500 m^3/h for both increasing and decreasing volume flow.

5.2.3 Summary and comparison

Table 5.2 presents the highest peaks for the three different operational points that have been studied in this sub chapter: 50, 100 and 500 m^3/h.

Amplitude	Frequency [Hz]	f [Hz]	Operational Point [m^3/h]
0.01611	2.73	45	50 (dec)
0.01133	2.87	45	100 (dec)
0.01368	4.00	45	500 (inc)
0.01085	2.79	45	50 (inc)
0.01082	2.22	40	50 (dec)
0.01044	2.12	40	100 (dec)
0.00745	1.84	35	100 (dec)
0.00738	1.79	25	50 (dec)
0.00738	1.79	35	50 (dec)
0.00692	4.24	45	500 (dec)
0.00647	1.97	45	50 (inc)
0.00637	1.40	30	100 (dec)
0.00542	4.88	35	50 (dec)
0.00538	4.90	25	50 (dec)
0.00529	2.00	40	500 (dec)
0.00488	0.42	25	500 (inc)
0.00484	1.36	35	500 (dec)
0.00484	0.96	45	500(inc)
0.00476	1.09	45	50 (dec)
0.00471	0.22	45	50 (inc)
0.00469	3.07	45	500 (inc)
0.00466	1.54	30	50 (dec)
0.00463	6.43	45	100 (dec)
0.00453	2.55	45	500 (dec)

Table 5.2: The highest peaks for all frequencies (f) sorted with the highest amplitude first. Dec means decreasing Q, while inc means increasing Q.

5.3 Results from the simulation program

This sub chapter will present the most important results from the simulation program. First of all, the volume coefficient is estimated, since this variable affects the frequency of the u-tube oscillations a lot. Both a simulation of the test-rig at TU, and a testing of the stability criteria is also given in this sub chapter.

5.3.1 Volume coefficient

Chapter 4.4 mentioned that the volume of the trapped air inside the pressure accumulator, was not measured. The idea with a volume coefficient was also mentioned, where a volume coefficient of 1 means that the accumulator is filled with air, and a volume coefficient of 0 means that the accumulator is filled with water.

The volume of the air has a big impact on the frequency of the simulated mass oscillations, and this is presented in table 5.3. The pressure used here is the maximum accumulator pressure for the five different frequencies f, and a volume coefficient of both 0.01 and 1 has been used in the calculation of the frequency in equation 3.8.

f [Hz]	Mass oscillations [Hz] Volume coefficient=0.01	Mass oscillations [Hz] Volume coefficient=1
25	17.3	1.77
30	17.6	1.79
35	17.8	1.81
40	18.0	1.84
45	18.3	1.87

Table 5.3: Calculated frequencies of the mass oscillations for two different volume coefficients: 0.01 and 1.

Different volume coefficients have been tested, in order to try to simulate the same frequencies as the two unknown peaks in figures 5.3 and 5.4. Table 5.4 presents these volume coefficients. The column in the middle is for the peaks around 4 Hz, and the column to the right is for the peaks around 2 Hz.

f [Hz]	Volume coefficient for peaks around 4 Hz	Volume coefficient for peaks around 2 Hz
25	0.18	0.76
30	0.19	0.79
35	0.20	0.81
40	0.20	0.83
45	0.21	0.86

Table 5.4: Calculated volume coefficients in order to reach the two highest peaks in figures 5.3 and 5.4.

For the peaks around 4 Hz, the volume coefficient is quite constant, which it should be for the mass oscillations. 0.19 is therefore assumed to be the volume coefficient, and it is used in the simulation program.

5.3.2   Results from simulations of the experimental set-up

The simulation program was explained in chapter 4.4, and this sub chapter presents the simulated results from the laboratory set-up. First the results with $H_{st} = 0$ m are presented, which was the case for the closed loop set-up in Berlin. All dimensions and initial pressure are from the experiments, and the pump characteristics are also fitted to the measured pump characteristics in figure 5.2. Figures 5.10, 5.11 and 5.12 show the oscillations of the net-power for $Q = 50$, 100 and 500 m^3/h respectively. The net-power is the power from the pump, given by the pump characteristic, minus the power losses in the system, given by the system characteristic.

Oscillations in the accumulator pressure show similar results as the oscillations in net-power when plotted for one frequency (f) at the time. If the pressure oscillations from the accumulator were to be plotted for all values of f in one figure, the oscillations do not show, because the oscillations are small compared to the difference in averaged pressure. For this reason, the oscillations in net-power are chosen here, since these figures show oscillations when all speeds of rotation are plotted in one figure.

Tables 5.5 and 5.7 presents the calculation of the stability criterion in equation 3.14, where a positive stability indicator means the criterion is fulfilled.

The simulated frequencies from the program, the measured frequencies from the experiments and the calculated frequencies are presented in figures 5.6, 5.8 and 5.9. They are not similar, but the result is not too bad!
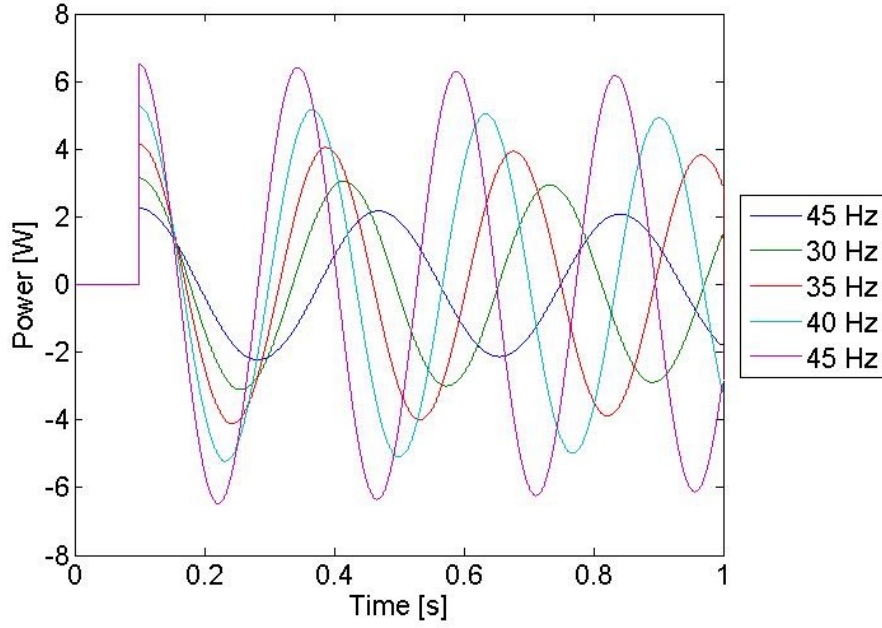
Figure 5.10: The oscillations in net-power [W] at $Q = 50$ m^3/h.

f [Hz]	dH_s/dQ	dH_p/dQ	$C \cdot 10^6$	Stability indicator
25	2356	20.34	0.159	0.014
30	3287	22.86	0.116	0.011
35	4345	26.10	0.096	0.011
40	5459	55.80	0.082	0.020
45	6768	63.00	0.069	0.019

Table 5.5: Calculation of the dynamic stability criterion seen in equation 3.14 at $Q = 50$ m^3/h. The stability indicator should be positive according to the criterion.

f [Hz]	Frequencies from simulation program [Hz]	Frequencies from experiment [Hz]	f_{u-tube} from equation 3.8 [Hz]
25	2.687	1.133	3.981
30	3.149	1.526	4.051
35	3.455	1.727	4.102
40	3.734	2.221	4.153
45	4.078	2.735	4.220

Table 5.6: The simulated, calculated and actual frequencies in Hz for different f at $Q = 50$ m^3/h.
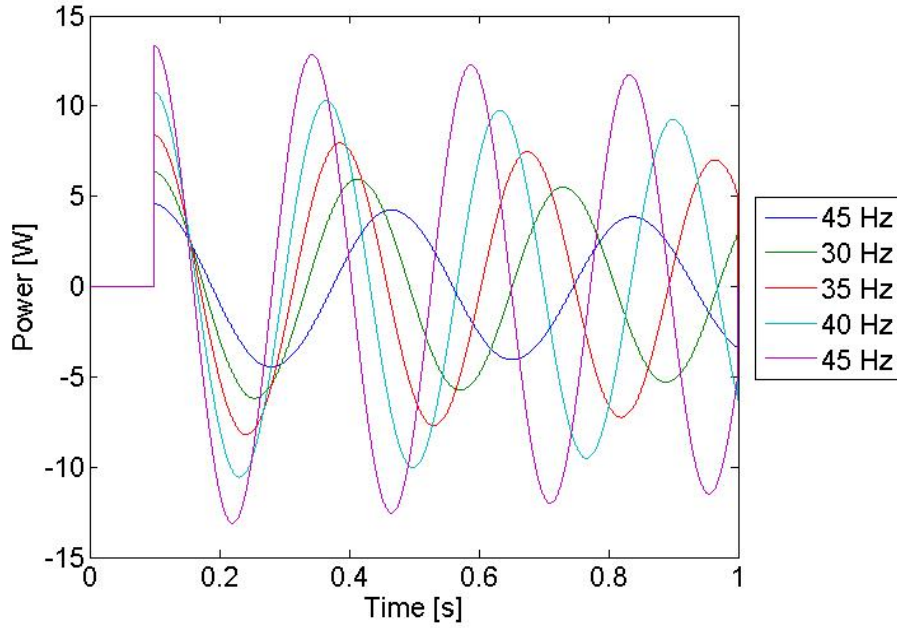
Figure 5.11: The oscillations in net-power [W] at $Q = 100$ m^3/h.

f [Hz]	dH_s/dQ	dH_p/dQ	$C \cdot 10^6$	Stability indicator
25	1193	9.540	0.159	0.006
30	1660	10.26	0.116	0.005
35	2192	13.50	0.096	0.005
40	2776	36.00	0.082	0.013
45	3438	45.00	0.069	0.013

Table 5.7: Calculation of the dynamic stability criterion seen in equation 3.14 at $Q = 100$ m^3/h. The stability indicator should be positive according to the criterion.

f [Hz]	Frequencies from simulation program [Hz]	Frequencies from experiment [Hz]	f_{u-tube} from equation 3.8 [Hz]
25	2.690	1.095	3.981
30	3.151	1.398	4.051
35	3.455	1.825	4.102
40	3.737	2.148	4.153
45	4.082	2.870	4.220

Table 5.8: The simulated, calculated and actual frequencies in Hz for different f at $Q = 100$ m^3/h.
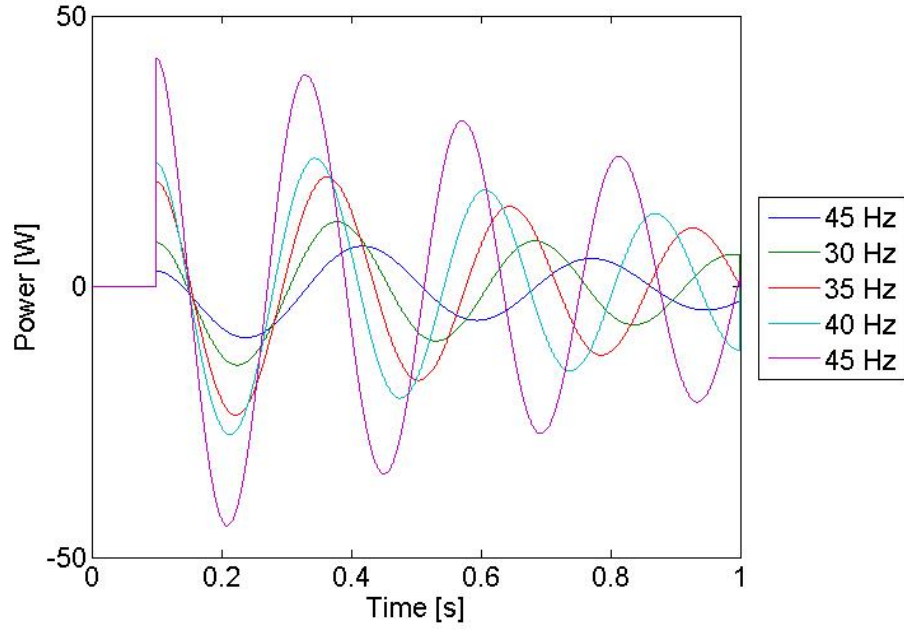
Figure 5.12: The oscillations in net-power [W] at $Q = 500$ m^3/h.

f [Hz]	Frequencies from simulation program [Hz]	Frequencies from experiment [Hz]	f_{u-tube} from equation 3.8 [Hz]
25	2.776	0.4211	3.981
30	3.234	0.4167	4.051
35	3.524	1.632	4.102
40	3.797	2.500	4.153
45	4.129	4.004	4.220

Table 5.9: The simulated, calculated and actual frequencies in Hz for different f at $Q = 500$ m^3/h.

5.3.3 Testing the static stability criteria

Sections 5.3.3 and 5.3.4 present the results from the tests of the stability criteria seen in chapter 3.4. Both the case where the distance between the pump and the accumulator is long, and the case where the distance between the accumulator and the valve is studied. For the first case, $L_1 = 0.5$ m and $L_2 = 10$ m, and afterwards they are switched so L_1 becomes the longest of them. Only the frequency where $f = 45$ Hz is studied here.

The static stability criterion given in equation 3.13, can be tested in the simulation program by increasing H_{st} to a high enough level. In figure 5.13, $H_{st} = 47$ m, which means the slope of the system characteristic is close to zero. L_2 is here the longest pipe, but the same result was also found when L_1 was the longer pipe.
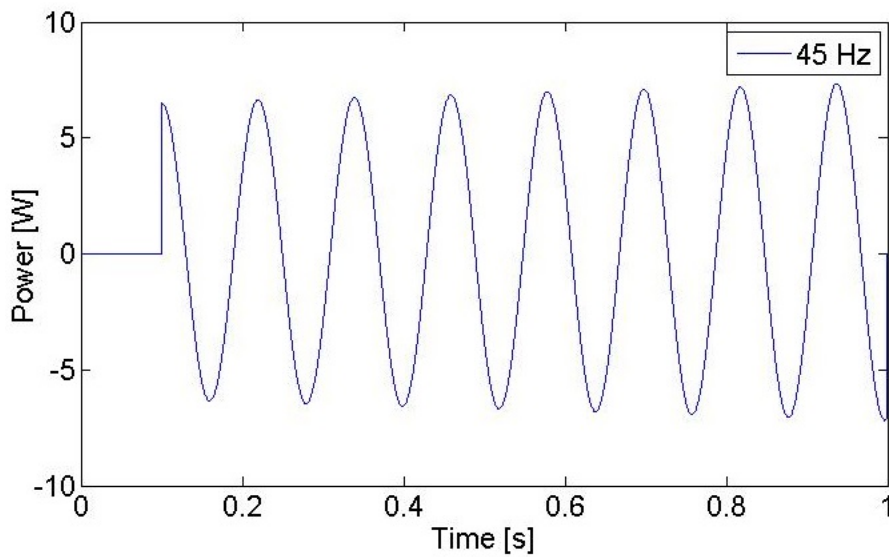
Figure 5.13: The results where $H_{st} = 47$ m, $Q = 50$ m^3/h, $L_1 = 0.5$ m and $L_2 = 10$ m.

5.3.4 Testing the dynamic stability criteria

The dynamic stability criterion, as seen in chapter 3.4, is tested in the simulation program. First the case where the accumulator is next to the valve, as seen in figure 3.10 is presented. L_1 is here set to 0.5 m and L_2 is set to 10 m in Matlab.

In figure 5.14, $H_{st} = 0$ m, which means the slope of the system characteristic is much steeper than the slope of the pump characteristic for $Q = 50$ m^3/h.
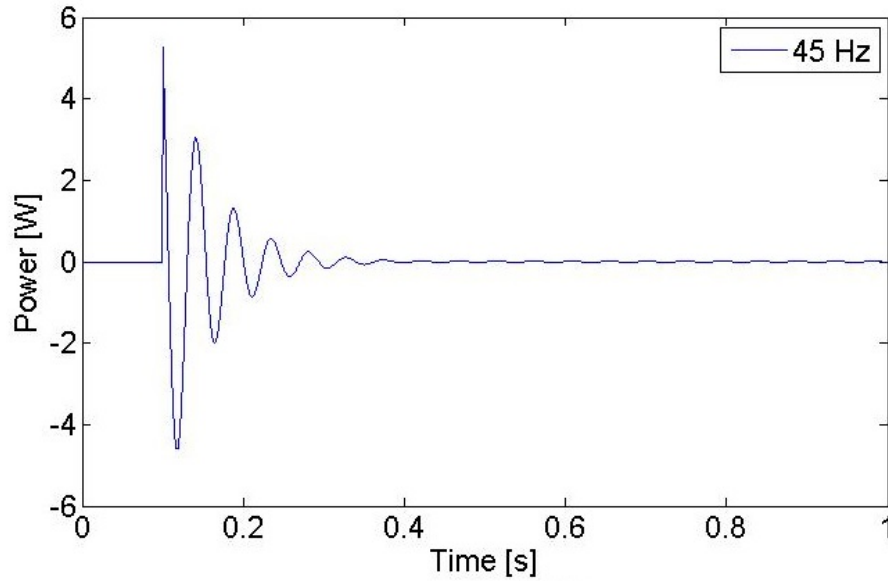
Figure 5.14: Testing the stability criteria for $H_{st} = 0$ m, $Q = 50$ m^3/h, $L_1 = 0.5$ m and $L_2 = 10$ m. It shows the oscillations in net-power.

Next the operational point is moved to the stable region of the pump characteristic, at $Q = 500$ m^3/h. The rest of the parameters are for now kept the same as in figure 5.14.
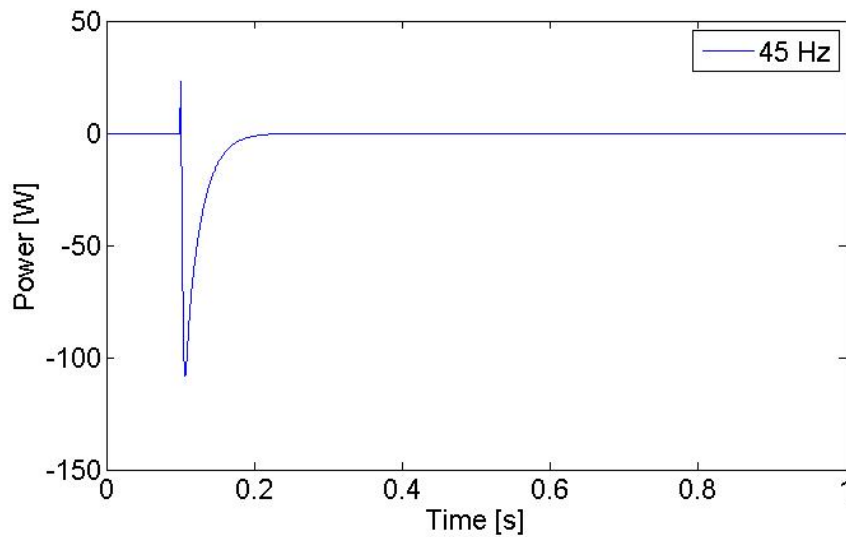
Figure 5.15: Testing the stability criteria for $H_{st} = 0$ m, $Q = 500$ m^3/h, $L_1 = 0.5$ m and $L_2 = 10$ m. It shows the oscillations in net-power.

In figure 5.16, $H_{st} = 20$ m, and the operational point is in the unstable region of the pump characteristic, at $Q = 50$ m^3/h. The case where $Q = 500$ m^3/h is presented in figure 5.17.
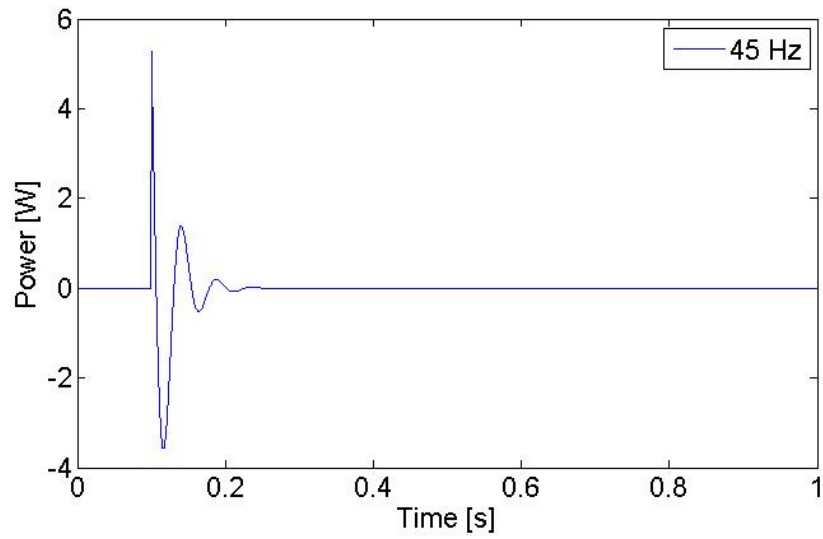
Figure 5.16: Testing the stability criteria for $H_{st} = 20$ m, $Q = 50$ m^3/h, $L_1 = 0.5$ m and $L_2 = 10$ m. It shows the oscillations in net-power.
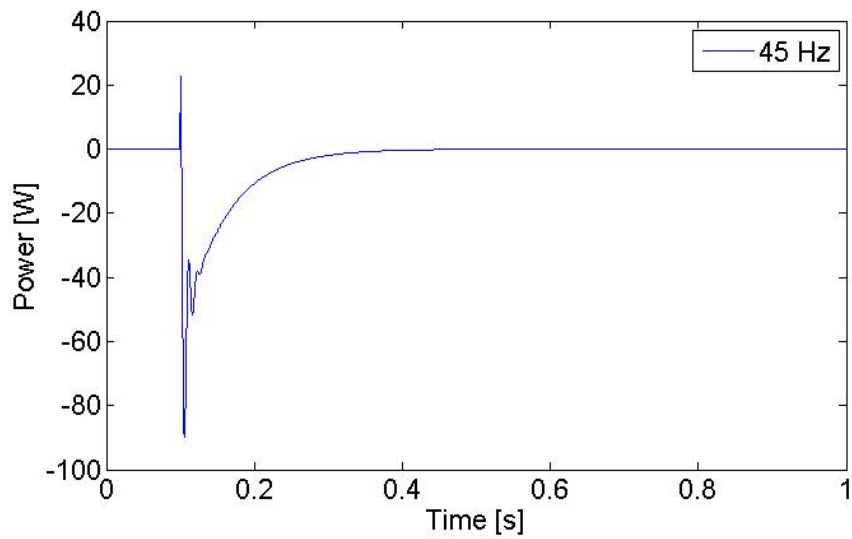
Figure 5.17: Testing the stability criteria for $H_{st} = 20$ m, $Q = 500$ m^3/h, $L_1 = 0.5$ m and $L_2 = 10$ m. It shows the oscillations in net-power.

Table 5.10 presents the calculated stability indicator for some operational points, where the indicator should be positive for stable operation according to equation 3.14. Both simulations of $H_{st} = 40$ m and $Q = 100$ m^3/h are also found in the table, even though the figures for these simulations are not presented.

Q [m³/h]	H_{st} [m]	Stability indicator
50	0	0.0037
50	20	0.0035
50	40	0.0028
100	0	0.0024
100	20	0.0022
100	40	0.0009
500	0	-0.0075
500	20	-0.0088
500	40	-0.0206

Table 5.10: A stability indication, calculated from equation 3.14 for different f, Q and H_{st} for the case where $L_1 = 0.5$ m and $L_2 = 10$ m.

Next the case where $L_1 = 10$ m and $L_2 = 0.5$ m is studied. According to sub chapter 3.4.3, the stability criterion is opposite here, and this is tested by looking at figures 5.18, 5.19, 5.20 and 5.21.

In figure 5.18, $H_{st} = 0$ m, which means the slope of the system characteristic is much steeper than the slope of the pump characteristic for $Q = 50$ m³/h.
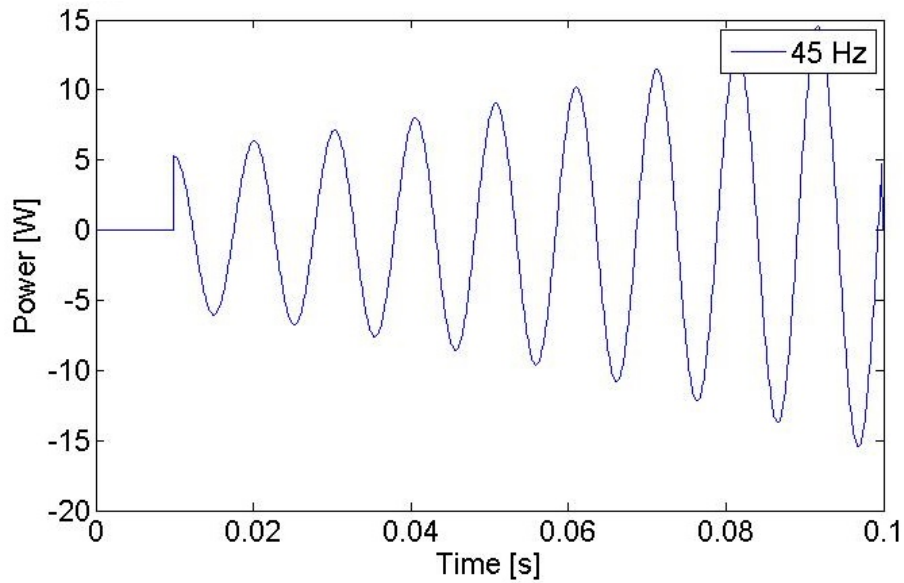
Figure 5.18: Testing the stability criteria for $H_{st} = 0$ m, $Q = 50$ m³/h, $L_1 = 10$ m and $L_2 = 0.5$ m. It shows the oscillations in net-power.

In figure 5.19, $H_{st} = 0$ m and $Q = 500$ m^3/h.
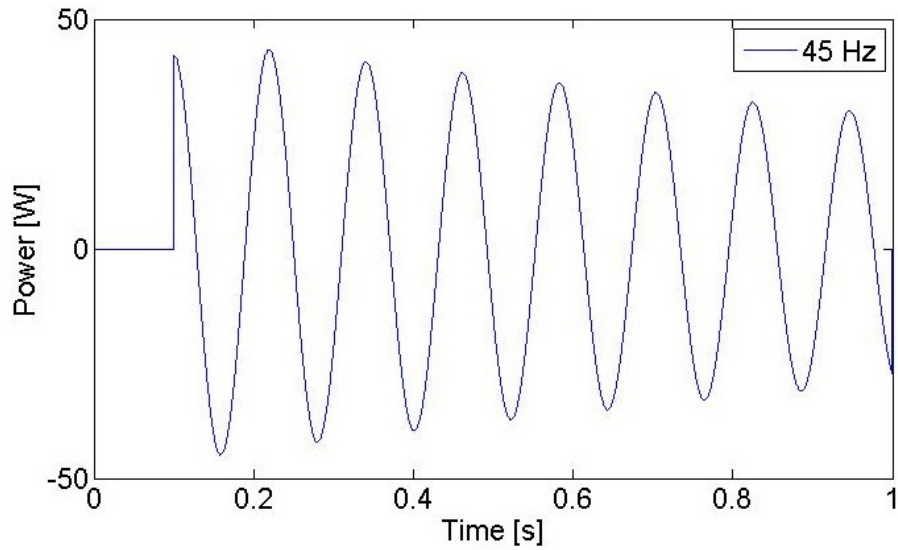
Figure 5.19: Testing the stability criteria for $H_{st} = 0$ m, $Q = 500$ m^3/h, $L_1 = 10$ m and $L_2 = 0.5$ m. It shows the oscillations in net-power.

Next, the case where $H_{st} =20$ m is studied. Figure 5.20 shows the operational point where $Q= 50$ m^3/h and figure 5.21 shows $Q= 500$ m^3/h.
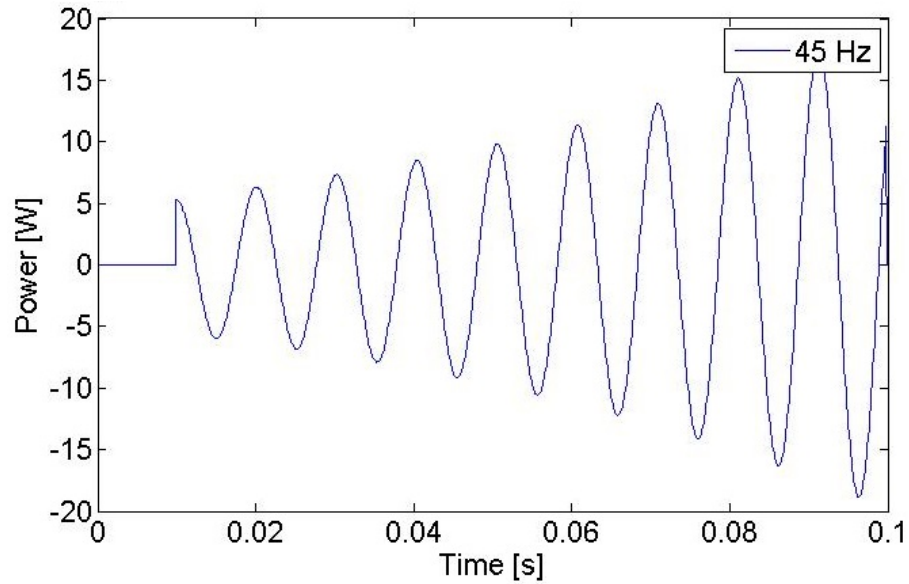
Figure 5.20: Testing the stability criteria for $H_{st} = 20$ m, $Q = 50$ m^3/h, $L_1 = 10$ m and $L_2 = 0.5$ m. It shows the oscillations in net-power.
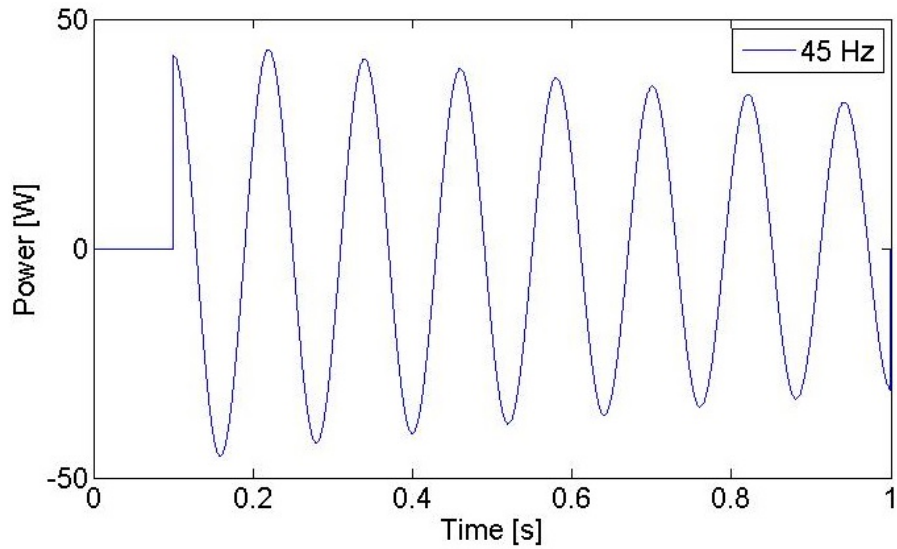
Figure 5.21: Testing the stability criteria for $H_{st} = 20$ m, $Q = 500$ m^3/h, $L_1 = 10$ m and $L_2 = 0.5$ m. It shows the oscillations in net-power.

Table 5.10 calculated the criterion given in equation 3.14. A similar table could be made for the cases simulated in figures 5.18, 5.19, 5.20 and 5.21, but the values would be equal and negative to the values in table 5.10. Such a table has therefore not been made for the case where the distance between the pump and accumulator is short.

Chapter 6

Discussion

This chapter discusses some of the aspects from chapter 5, and also why the laboratory set-up at TU was not ideal for verifying the stability criteria. The results consist of both the pump characteristics, the pressure inside the accumulator and graphs from the simulation program, and they are discussed in sub chapter 6.1. The two stability criteria and the problems with verifying them are discussed in sub chapter 6.2.

6.1 Discussion of the results

This sub chapter focuses on the results from chapter 5, but first one general remark is given.

One of the biggest sources of error is that no calibration data are available for the sensors used in this Master's Thesis. There was no time to calibrate the sensors after arrival in Berlin, and the attempt to get hold of the data failed. This is of course unfortunate, since it means that the measured values cannot completely be trusted. The lack of calibration data also affects the uncertainty analysis, which ideally should have calculated the uncertainty of the measurements. Even though this makes the results less trustworthy, there are other problems of much greater concern when it comes to verification of the stability criteria.

6.1.1 The pump characteristic

Figure 5.1 plots all the measured pump characteristics, showing that not all pump characteristics are consistent. This could imply hysteresis, but it could also be that some of the measurements were saved too quickly. The least consistent measurement is at $f = 45$ Hz, and this was done fast to limit the increase in temperature. The 25 Hz curve shows very similar results for the two executed measurements, and it is therefore assumed that hysteresis does not make the two 45 Hz measurement differ much.

The averaged pump characteristics in figure 5.2 seem trustworthy, because the shapes of the pump characteristics look quite similar. The head delivered by the pump increases with speed of rotation, as it should according to figure 3.4.

6.1.2 The pressure accumulator

The results from the pressure accumulator were presented in section 5.2, and they consist mostly of plots of Fourier transforms from the pressure accumulator. Some of the peaks in figures 5.3–5.9 have already been explained in chapter 5.2. Both the rotational frequency and the water hammer frequency are found, but there are two peaks that are not fully accounted for, where no harmonic connection is found between them. One of the peaks is found at around 2 Hz and other one around 4 Hz, and one of these peaks is assumed to originate from the mass oscillations.

The rotational frequency, f_{rot}, calculated in table 4.2, is only found for the 40 Hz and the 30 Hz. One of the reasons for this might be the large damping in the junction between the main pipe and the pressure accumulator. Some of the frequencies might have been dampen more than the others, but it is still strange they did not show in the plots.

Figure 5.6 presents the result for $Q = 100$ m^3/h and $f = 45$ Hz for both increasing and decreasing volume flow, and the two curves are quite similar. The amplitude of the peaks varies, but the frequency coincides. This is also the case in figure 5.9, where $Q = 500$ m^3/h and $f = 45$ Hz is studied for both increasing and decreasing volume flow. A comparison of figures 5.7 and 5.8, which presents $Q = 500$ m^3/h for all frequencies f for decreasing and increasing volume flow respectively, show less degree of agreement. The biggest difference between them is the frequencies around 0.25 Hz seen in figure 5.7. These are assumed to be noise, since they are not present in figure 5.8.

The pressure sensor at the top of the accumulator was set to take 100 samples per second. Here the studied frequencies are the u-tube oscillations, which oscillate with a frequency less than 20 Hz. It is recommended to have a sampling frequency at least twice the frequency of interest, so the sensor is taking enough samples to detect the mass oscillations.

The sampling rate was unfortunately too small to detect the runner blade frequency though. These frequencies vary between 75 and 135 Hz according to equation 3.22, but the maximum frequency in the plots is 50 Hz. This is because the integrated function in Matlab, that did the Fourier transformations, did not include frequencies over two times the sampling rate. In this Master's Thesis the runner blade frequency is not very important, but it would have been a nice insurance to observe it in the plots, and the sampling rate should then have been larger.

The Fourier transform means that an assumption on periodic waves has been made, as was mentioned in chapter 4.2.3. Periodic waves are not necessarily the case, which might explain some of the unexplained frequencies and noise seen in the figures 5.3 – 5.9

Table 5.2 presents the highest peaks in the figures 5.3 – 5.9. The peaks between 1.79 and 2.87 Hz give the highest amplitude, except the point for $Q = 500$ m^3/h. The amplitude of the oscillations between 1.79 and 2.87 Hz are large for the unstable operating points ($Q = 50$ and 100 m^3/h), and are larger for high speed of rotation than small speed of rotation. They may therefore be connected to the unstable pump characteristic, and unstable operation of the pump may then have been accomplished.

In table 5.2, it is also possible to see some peaks around 4 Hz. They have highest amplitude where $Q = 500$ m^3/h and $f = 45$ Hz for both increasing and decreasing volume flows.

Neither of the two peaks coincide with the rotational frequency of the pump. No other sources known to cause vibrations in pumps have jet been found, except the frequency of the mass oscillations mentioned above. The frequency of the mass oscillations should increase with both increasing pressure and decreasing volume of the air in the accumulator, because this would decrease the time it takes filling the accumulator. This implies the mass oscillations to be at its highest at $f = 45$ Hz and the operational point at the top of the pump characteristic, which is the case for the peaks around 2 Hz in table 5.2. On the other hand, the valve is almost closed for small Q, and the u-tube oscillations are then assumed to be dampen here. The mass oscillations are further discussed in the next sub chapter.

6.1.3 The simulation program

This section's focus is the reliability of the simulation program. Whether or not the experiments were able to verify the stability criteria is further discussed in section 6.2.1.

The simulation program uses Euler's method to solve the differential equations from chapter 3.3, see equations A.2 to A.4. Most of the parameters in these equations were measured, except the already mentioned air volume. The volume was therefore estimated with the help of the dimensions of the accumulator. Table 5.3 presents the calculated frequencies of the mass oscillations for a volume coefficient of both 0.01 and 1. A volume coefficient of 0.01 means the accumulator is almost filled with water, which gave a maximum frequency of 18.3 Hz. The volume coefficient when the accumulator is filled with air is 1, and table 5.3 shows that this gives a simulated frequency of minimum 1.77 Hz. For some values of f, the Fourier transform shows several peaks inside this domain. It is therefore not that easy to understand which peaks originate from the mass-oscillations.

Table 5.4 presents the calculated volume coefficients that simulate both the peaks around 2 and 4 Hz in figures 5.3 and 5.4. The accumulator pressure used in the simulation, is the pressure where Q is at its maximum at the given frequency. Both the volume coefficients for the peaks around 2 Hz and the peaks around 4 Hz are possible, because all volume coefficients seen in the table are between 0 and 1. The calculated volume coefficients for the peaks around 4 Hz show very similar results, approximately around 0.19, and this is thus assumed to be the volume coefficient. V_0 in equation 3.6 is then the volume of the accumulator, $A_{acc} \cdot L_{acc}$, multiplied with 0.19, while $H_{acc,0}$ is the maximum accumulator pressure for the different frequencies f, divided by gρ.

Chapter 5.3 presented the simulations of the net-power for the laboratory set-up. All figures 5.10, 5.11 and 5.12 showed stable operation, and both these observations, and tables 5.5 and 5.7, are further discussed in chapter 6.2.1. Here, the frequency and the amplitude of the oscillations in these figures are discussed. Figures 5.10, 5.11 and 5.12 all show that the period is smaller at the biggest frequency. The frequencies of the mass

oscillations are therefore biggest at $f = 45$ Hz. This is also the results from the measurements, which is for example seen in figure 5.3. The highest amplitude of the oscillations is at $f = 45$ Hz. This makes sense, because the power input from the pump is bigger for high frequencies.

The assumption of ideal gas, and adiabatic and reversible compression process, mentioned in chapter 3.3, may be incorrect. This influences the results from the simulation program, so they are wrong compared to the results from the pressure accumulator.

Tables 5.6, 5.8 and 5.9 compares the simulated, measured and calculated frequencies. All the frequencies are below 5 Hz, and some of them coincides very well. All three frequencies are increasing with f, but the simulated frequencies are covering a bigger range of frequencies, starting from approximately 2.6 Hz for $f = 25$ Hz, and ending at around 4.1 Hz for $f = 45$ Hz. The measured frequencies vary more, and a clear trend is not that easy to see. f_{u-tube} varies between 3.9 Hz and 4.2 Hz, and has a smaller variation than the simulated values.

It is not that easy to simulate mass oscillations, because there are many factors affecting them. The simulation program do, however, show promising results, and the program could then be used to test the stability criteria for both the laboratory set-up, and the systems seen in figures 3.10 and 3.11. The next sub chapter will discuss the results from these simulations, and also why the verification at TU did not go as planned.

6.2 The stability criteria

6.2.1 The stability criteria for the laboratory set-up

The laboratory set-up, seen in figure 4.1, is neither of the two systems in figures 3.10 and 3.11. At TU, the distance between the pump and the accumulator is smaller than from the accumulator to the valve, thus more equal to the system in figure 3.11. It is not easy to know which sets of criterion to follow though, and both of the criteria are therefore discussed in this section.

In order to test the static stability criterion in equation 3.13, it is important to have a static head. This is not possible in the closed-loop set-up used here, since this means the static head is zero. The fact that the closed loop would be a problem, did not become evident before starting to run the tests at TU. There was then no time to change the set-up of the laboratory. Ideally the system should have two reservoirs with the possibility of changing H_{st}. It is also possible to change the speed of rotation instead of the static head. The static head has to be higher than zero in order to reduce the speed of rotation enough. If the static head is too small, it is impossible to enter the unstable region, and at the same time have an almost flat system characteristic.

In equation 3.17, a completely different static stability criterion is given. For this criterion, a low H_{st} is negative for stability, and the criterion is violated for all operating points in the unstable region of the pump characteristic. Which of the two criteria seen

in equations 3.13 and 3.17 are more correct for the experiments is not evident.

The energy storage capacity of the system is important when it comes down to dynamic stability, as mentioned in chapter 3.4. In order to test this, either the pressure in the accumulator or the volume should be easier to vary. The set-up used in this Master's Thesis, makes it possible to decrease the pressure in the accumulator by opening a valve at the top of the accumulator. An increase in pressure may be more difficult. If there is room for more water in the big tank, filling it increases the pressure in the accumulator. If the big tank is full, the maximum pressure in the accumulator is reached.

Figures 5.10, 5.11 and 5.12 presented the simulation of the set-up, and they all showed stable behaviour. The simulation program is very simplistic though, and it is not a good idea to trust it completely. The first of these figures, figure 5.10, is the case for $Q = 50$ m^3/h, and this figure shows dynamic stable behaviour for frequencies. Table 5.5 presents the slopes of both the pump- and system characteristics, the compliance C, and the calculation of equation 3.14. This was also tested for $Q = 100$ m^3/h, and the result is seen in figure 5.11 and table 5.7. All the calculated stability indicators are positive, but just barely, which means the criterion in equation 3.14 is fulfilled. This also means the opposite criteria seen in equation 3.19 is violated, since this criteria would give the same values as in tables 5.5 and 5.7, but negative.

The stable operating point where $Q = 500$ m^3/h is presented in figure 5.12, and this figure shows a stable operation for all frequencies. This is expected behaviour, but if the criterion in equation 3.14 is calculated though, it becomes negative, since the slope of the pump characteristic is negative. Operating points in the stable region of the pump characteristic is according to the literature always stable, as mentioned in chapter 3.4, and the criterion is then assumed to not be valid for negative $\mathrm{d}H_p/\mathrm{d}Q$.

The cross sectional area of the pipe between the main pipe and the pressure accumulator, is very small. This is assumed to give big losses, which again leads to increased damping and increased stability. The narrow junction thus makes it more difficult to set the pump in a predicted unstable operation. The stabilizing effect of the junction loss in turbine mode was mentioned in chapter 3.3.

This section has tried to show that is not straightforward to decide whether or not the pump was set in an unstable behaviour. During the experiments, a lot of vibrations and noise in pipes and pump took place, but this was the case for all volume flows. The water level inside the accumulator was shaking, and it looked as though it was because of the oscillations. Figures 5.3 and 5.4 do show high amplitudes around 2 Hz, and these oscillations might be because the pump was set in an unstable behaviour. Anyhow, a verification of the stability criteria did not take place, because in order to test a criteria, all the parameters should be easy to vary. This was not the case at TU, and especially the lack of static head made the verification difficult. A suggestion for a new laboratory set-up is therefore seen in sub chapter 6.3.

6.2.2 The static stability criteria

Both stability criteria in equations 3.14 and 3.19 were tested in Matlab. Figure 5.13 is for the system seen in figure 3.10 for a very large H_{st}, so the slope of the system characteristic became zero, and it shows unstable behaviour. A simulation was also performed for the case in figure 3.11, and it showed an equal behaviour to figure 5.13.

The different pump books and articles read during the Master period seems to agree in the static stability criterion seen in equation 3.13. For the stability criterion in equation 3.17, none sources except Anderson [6] are found. This is further discussed in the next section.

6.2.3 The dynamic stability criteria

Sub chapters 3.4.2 and 3.4.3 give the dynamic stability criteria for two simplified systems consisting of discrete inertia and elasticity. The two figures 3.10 and 3.11 give different criteria, and these were tested in the simulation program.

First, the case for long pipe between pump and accumulator is discussed. The dynamic stability criterion for this case is found in equation 3.14, and it states that a too flat pump characteristic is not good for stability. Ideally, the pipe should be wide and short, and the elastic compliance big for stability. These parameters were unfortunate not tested properly, because of lack of time. A steep valve characteristic is also good for stability, and this was tested.

Figures 5.14 – 5.17 presents the case where the length between pipe and accumulator is long. For figures 5.14 and 5.15, $H_{st} = 0$ m, and the results are stable for both figures. When $H_{st} = 0$ m, the slope of the valve characteristic is very steep, which can explain the stable operation. Figures 5.16 and 5.17, where $H_{st} = 20$ m, also show stable operation.

Table 5.10 show the difference between the left and the right side of the inequality in equation 3.14, and this difference is called a stability indicator. For $Q = 50$ and 100 m^3/h, the stability indicator is positive (which indicates stability), while for $Q = 500$ m^3/h the stability indicator is negative. $Q = 500$ m^3/h is in the stable region of the pump characteristic, and instabilities should not occur here, according to chapter 3.4. Equation 3.14 is therefore assumed to only be valid for the unstable region of the pump characteristic. The stability indicator for $Q = 50$ and 100 m^3/h, agrees with figures 5.14 and 5.16, meaning the simulation program agrees with the stability criteria in equation 3.14.

Next, the case for a long pipe between the accumulator and the valve, is discussed. The results are seen in figures 5.18 – 5.21. Both figures where $Q = 50$ m^3/h, show unstable operation, while for $Q = 500$ m^3/h, the behaviour are stable. Here, the dynamic criterion is given in equation 3.19, and it is the opposite criterion to the one in equation 3.14. A very steep system characteristic at $Q = 50$ m^3/h is therefore here negative for stability. Also here, the simulation program seems to agree with the stability criteria.

The figures discussed above show very different results for the two different combina-

tions of lengths, and the simulation program thus agrees with chapter 3.4 and the idea with two different sets of criteria. The article by Anderson called "Simple first-order models for surging in pumps and compressor systems" [6] is the only source of information found in this Master's Thesis who mentions this as a possibility, and this is a bit strange. One of the reason for this might of course be that the results from the article are wrong. Another possibility is that the accumulator usually is placed next to the valve for pumping systems, thus needing only one set of criteria.

Rothe and Rundstadler Jr. did a similar experiment to the one executed in this Master's Thesis, which they presented in the article "First Order Pump Surge Behavior" [10]. The results from their tests corresponded with available theory at the time, and they observed more oscillations in the unstable region than in the stable region. The laboratory set-up used in their experiment was a closed-loop, and the valve was placed straight after the accumulator. This experiment was thus similar to the one seen in figure 3.10, which gives the most common stability criteria. From their point of view, simple first-order equations seems to be able to foresee the unstable behaviour of pumps.

6.3   Ideas for a new experimental set-up

This sub chapter will try to summarize some of the issues that have been discussed up to now.

First of all, the valve, the frequency converter and the ability to handle large vibrations, was some of the advantages from the set-up at TU, and they should also be included in the next laboratory set-up.

The ability to vary H_{st} is necessary in order to verify equation 3.13. It would also be a big advantage when it comes to verifying the dynamic criteria given in equations 3.14 and 3.19. A measurement of the trapped air inside the accumulator would also have been useful, because it would improve the simulations a lot.

Ideally, the position of either the accumulator or the valve should be possible to vary. Only then is it possible to see if there really is a difference in stability criteria for the systems seen in figures 3.10 and 3.11.

In the experiments executed by Rothe and Rundstadler Jr. [10], a pump with $\beta > 90^0$ was used, consequently with unstable pump characteristic for a large range of operational points. They also had the possibility to vary the amount of trapped air inside the accumulator. Both these factors would have been a good idea in this experiment as well!

Hopefully, the experiences from this Master's Thesis will make it easier to verify the stability criteria next time!

Chapter 7

Conclusion

The objective of this Master's Thesis has been to verify the stability criteria for a centrifugal pump. Consequently, experiments on a centrifugal pump, which is unstable for some volume flows, were performed at the Technical University Berlin (TU). A simulation program made in the candidate's Project Thesis was also rewritten to simulate the pump rig at TU, and to test the stability criteria.

The stability criteria depend on both the pressure delivered by the pump and the pump's surrounding system. If the stability criteria is violated, the water in the system around the pump is affected. As a result, a small perturbation will lead to either exponential or oscillatory unstable behaviour of the water, and this is off course unwanted. Two different sets of criteria are found in the literature, both consisting of a static criterion and a dynamic criterion.

Verification of the stability criteria was not as straightforward as one have hoped. One of the issues was the pump itself, and it would have been easier with an even more unstable pump. In order to test a criterion, it is important to be able to change all the parameters supposedly influencing the stability. Many of the parameters were possible to vary, but unfortunately the laboratory set-up at TU was not able to meet the requirements.

The experiments were interesting and educational, even though the verification of the stability criteria did not go as planned. Experiments were done, and the candidate got to assist with installation of both a pressure sensor and the pressure accumulator.

The simulation program made in the candidate's Project Thesis, which simulates mass oscillations, was improved and adjusted to the laboratory in Berlin. It solves differential equations with Euler's method, and plots the results. In addition to simulating the existing lab, the simulation program made it possible to change the different parameters in the stability criteria. The mass oscillations are not easy to simulate, especially without knowing the volume of the air in the pressure accumulator-even though the results from the simulation program show similar results relative to the measurements. The simulation program also seemed to verify the stability criteria.

Chapter 8

Further work

It would be interesting to build a set-up that makes it easier to test the stability criteria. Two reservoirs with the possibility of varying the head between them, would be the best. Ideally the volume and the pressure in the accumulator, and the speed of rotation of the pump, should also be possible to change, see chapter 6.2. This was possible to a certain degree in the set-up used in this Thesis, but high pressure in the accumulator makes the water level too low, so air will come into the main pipe.

It is planned to build a test rig at the Waterpower Laboratory, for testing of u-tube oscillations. This might be possible to test for a centrifugal pump, if the set-up has room for a valve and a centrifugal pump.

Advantageously the pump could have an even more unstable pump characteristic. Precise prediction of the pump characteristic is not always easy, so the possibility of rapid prototyping of small pump impellers would be interesting. The Waterpower laboratory has in fact already a 3D printer, which makes it possible to print small objects in plastic. This could maybe be used for this purpose. A pump with back bent blades would also be a good idea, because this makes the slope of the pump characteristic positive for a bigger region.

The simulation program could be made much more advanced, in order to better predict the mass oscillations. This would have been easier, if the volume of the compressed air was measured during the experiment. It is also possible that programs made by other students at the Waterpower Laboratory, can quite easily be rewritten to simulate pump instabilities.

Bibliography

[1] Hermod Brekke. *Pumper og Turbiner*. Water Power Laboratory, NTNU, 2003.

[2] Torbjørn K. Nielsen and Grunde Olimstad. Dynamic behavoiur of reversible pump-turbines in turbine mode of operation. 2010.

[3] J. Tuzson. *Centrifugal Pump Design*. Wiley, 2000.

[4] Hermod Brekke. *Grunnkurs i hydrauliske Strømningsmaskiner*. Water Power Laboratory, NTNU, 2000.

[5] Greitzer EM. The stability of pumping systems—the 1980 freeman scholar lecture. *Journals of Fluids Engineering*, 103:193–242, June 1981.

[6] A Anderson. Simple first-order models for surging in pump and compressor systems. *Proceedings of the Institution of Mechanical Engineers, Part C: Journal of Mechanical Engineering Science*, 209(3):149–154, 1995.

[7] Johann Friedrich Gülich. *Centrifugal Pumps*. Springer, 2nd edition, 2010.

[8] P. Dörfler, M. Sick, and A. Coutu. *Flow-Induced Pulsation and Vibration in Hydroelectric Machinery: Engineers Guidebook for Planning, Design and Troubleshooting*. Springer, 2012.

[9] A.J. Stepanoff. *Centrifugal and axial flow pumps: theory, design, and application*. Wiley, 1957.

[10] P. H. Rothe and P. W. Runstadler Jr. First-order pump surge behavior. *Journal of Fluids Engineering*, 100:459–466, 12 1978.

[11] J.G. Levine. *Large Energy Storage Systems Handbook*. Mechanical and Aerospace Engineering Series. Taylor & Francis, 2011.

[12] Thomas Staubli, Christian Widmer, Thomas Tresch, and Manfred Sallaberger. Starting pump-turbines with unstable characteristics. 2010.

[13] R.S. Stelzer, R.N. Walters, Engineering, and Research Center (U.S.). *Estimating Reversible Pump-turbine Characteristics*. Department of the Interior, Bureau of Reclamation, Engineering and Research Center, 1977.

[14] Sverre Stefanussen Foslie. Design of centrifugal pump for produced water. Master's thesis, NTNU, 12 2013.

[15] A Anderson. Surge shaft stability with pumpe-storage schemes. *Journal of Fluids Engineering*, 110(6):687–706, 1984.

[16] Z Zhang. Rotating stall mechanism and stability control in the pump flows. *IOP Conference Series: Earth and Environmental Science*, 12(1):012010, 2010.

[17] C.E. Brennen. *Hydrodynamics of Pumps*. Cambridge University Press, 2011.

[18] Hongjuan Ran, Xianwu Luo, Lei Zhu, Yao Zhang, Xin Wang, and Hongyuan Xu. Experimental study of the pressure fluctuations in a pump turbine at large partial flow conditions. *Chinese Journal of Mechanical Engineering*, 25(6):1205–1209, 2012.

[19] Frank M. White. *Fluid Mechanics*. McGraw-Hill, 6th edition, 2009.

[20] Torbjørn Nielsen. *Dynamisk dimensjonering av vannkraftverk*. Water Power Laboratory, NTNU, 1990.

[21] G.K. McMillan. *Centrifugal and Axial Compressor Control*. Momentum Press, 2010.

[22] Jeffrey Peter Bons. Instabilities and unsteady flows in centrifugal pumps. Master's thesis, Massachusetts Institute of Technology. Dept. of Aeronautics and Astronautics, 1990.

[23] *ISO9906 Rotodynamic pumps - Hydraulic performance acceptance tests - Grades 1, 2 and 3*, second edition, 2012.

[24] Einar Kobro. Trykkpulsasjoner i francisturbiner. Master's thesis, NTNU, 2006.

[25] Rakel Ellingsen. Reversible pump turbines - stability in pump mode. Project thesis, NTNU, 12 2013.

Appendix A

Data used in the simulation program

Equation A.1 calculates different shapes of pump characteristics when a change in variables occur.

$$Hp = H0 - aQ - bQ^2 - c(Q - Q^*)^2 \qquad (A.1)$$

The values a, b, c, Q^* and H0 seen in table A.1, give similar pump characteristics as those measured in Berlin, when used in equation A.1.

Frequency [Hz]	a	b	c	H0 [m]	Q^* [m^3/h]
25	0.00005	0.000015	0.000015	17.3	290
30	0.00005	0.00002	0.000015	24.1	330
35	0.00005	0.00002	0.000015	31.7	360
40	0.000001	0.00003	0.000025	41.4	420
45	0.000001	0.000025	0.000025	51.1	450

Table A.1: Values for a, b, c, H0 and Q* that, combined with equation A.1, will simulate the measured pump characteristics.

Table A.2 gives the initial pressures and volume coefficients used in the simulation program. The p0 values are the pressure inside the accumulator when the valve is open. Hp0, which is the pressure in the accumulator in meter, is the p0 values divided by g and ρ. The volume coefficient has been found by testing many values, in order to try to match the frequency of the oscillations in the program with the frequencies measured in Berlin.

Frequency [Hz]	p0 [Pa]	Hp0 [m]	Volume coefficient
25	112000	11.42	0.96
30	116000	11.82	0.78
35	119000	12.13	0.56
40	122000	12.44	0.38
45	126000	12.84	0.26

Table A.2: The values for p0, Hp0 and the volume coefficient used in the simulation program.

The equations solved with Euler's in Matlab are equations 3.2 to 3.4. This means that the equations are solved as they are displayed in equations A.2 to A.4. Δt is here a small time step called deltat in Matlab. n is the time interval, so n+1 means next interval in time, while n means the previous one.

$$Q_1^{n+1} = Q_1^n + \frac{gA_1}{L_1}\Delta t(\frac{p_{acc}}{\rho g} - H_{st} - k(Q_1^n)^2 + loss) \tag{A.2}$$

$$Q_2^{n+1} = Q_2^n + \frac{gA_2}{L_2}\Delta t(H_p - \frac{p_{acc}}{\rho g} - loss) \tag{A.3}$$

$$p_{acc}^{n+1} = p_{acc}^n + \frac{g\rho}{3600A_{eq}}\Delta t(Q_2^n - Q_1^n) \tag{A.4}$$

Appendix B

Matlab source code

```matlab
1  clc;
2  clear all;
3  hold on
4
5  %Reads the constant for the pump characteristics from Excel
6  a=xlsread('Frekvenskalkulasjon.xlsx','H14:H18');
7  b=xlsread('Frekvenskalkulasjon.xlsx','I14:I18');
8  c=xlsread('Frekvenskalkulasjon.xlsx','J14:J18');
9  H0=xlsread('Frekvenskalkulasjon.xlsx','K14:K18');
10 Qstar=xlsread('Frekvenskalkulasjon.xlsx','L14:L18');
11
12 %Constants and dimensions
13 g=9.81;
14 rho=1000;
15 D=0.34;
16 A=(D/2)^2*pi;
17 L1=8;          %Length between accumulator and valve, approximately 8
      meters
18 L2=2;          %Length between pump and accumulator, approximately 2
      meters
19 kappa=1.4;
20 L_acc=0.6;
21 A_acc=0.0201;
22 %As_test=0.0001;
23
24 %The statical head. It is zero in the experiment. Can be changed to
      see what effect the static head has on the stability
25 Hst=0;
26
27 %Decides the maximum time and the time steps
28 tmax=1;
29 deltat=0.0001;
30
31 %Read values for pressure and volume exponent from Excel
32 %B:50, C:100, D:150, E:200, F:250, G:300, H:350, I:400, J:500
```

```matlab
33  P1=(xlsread('Frekvenskalkulasjon.xlsx','B21:B25')-1.01300)*10^5*10;
34  volumeexp=ones(5,1)*0.198;
35  p0=xlsread('Frekvenskalkulasjon.xlsx','B14:B18')-101300;
36
37  %Calculates the equivalent area and the frequencies of the mass
         oscillations
38  helmholtz=zeros(1,length(P1));
39  As=helmholtz;
40  Va=L_acc*A_acc*volumeexp;
41  for i=1:length(Va)
42      helmholtz(i)=sqrt(A*kappa/(rho*L1)*P1(i)/Va(i))/(2*pi());
43      As(i)=1/(1/A_acc+P1(i)*kappa/(g*rho*Va(i)));
44      f_torb(i)=sqrt(g*A/(As(i)*L1))/(2*pi());
45  end
46
47  %The pump characteristics are plotted so it is easier to decide which
         operating point to study
48  x=(0:0.1:1000);
49  Q_plot= repmat(x,length(H0),1);
50  Hp_plot=zeros(length(H0),length(Q_plot));
51   for i=1:length(Q_plot)
52      for j=1:length(H0)
53          Hp_plot(j,i)=H0(j)-a(j)*Q_plot(j,i)-b(j)*(Q_plot(j,i))^2-c(j
                )*(Q_plot(j,i)-Qstar(j))^2;
54      end
55   end
56
57  %The plot of the pump characteristics
58  figure(1)
59  plot(Q_plot',Hp_plot')
60  xlabel('Volume flow Q [m^3/h]')
61  ylabel('Head Hp [m]')
62  legend('25 Hz','30 Hz','35 Hz','40 Hz','45 Hz')
63
64  %The operational point is chosen through the command window
65  Q0=input('What Q0 [m^3/h] do you want to study?  ');
66
67  %Here is the start pressure decided. This is found with the help of
         the pump characteristics and the operational point.
68  Hp_Q0=zeros(5,1);
69  for i=1:5
70      Hp_Q0(i)=H0(i)-a(i)*Q0-b(i)*Q0^2-c(i)*(Qstar(i)-Q0).^2;
71  end
72
73  %The slope of the pump characteristic and the slope of the system
         characteristic is calculated next. This is done by the help of
         differentiation of the equations of the characteristics. k is the
         loss coefficient
74  Pp=(-a-2*Q0*b-2*Q0*c+2*diag(c)*Qstar)*3600;     %[1/ms]
```

```matlab
75  k=(Hp_Q0−Hst)/Q0^2;
76  Pt=(2*k*Q0)*3600;                              %[m^3/s^2]
77
78  %Figure 2 plots the characteristics and the operational point
79  figure(2)
80  plot(Q_plot',Hp_plot',Q0,Hst+k*Q0^2,'ko')
81  xlabel('Volume flow Q [m^3/h]')
82  ylabel('Head Hp [m]')
83  legend('25 Hz','30 Hz','35 Hz','40 Hz','45 Hz','Operational point','
        Location','SouthWest')
84
85  %Greitzer's dynamic stability criteria is calculated next. If
        posisstable is positive: stable according to Greizer's criteria
86  C=zeros(5,1);
87  for i=1:5
88      C(i)=(kappa*p0(i)/Va(i))^(−1);
89  end
90
91  posisstable=zeros(5,1);
92  for i=1:5
93      posisstable(i)=Pp(i)*A*g^2/L2*C(i)*rho−1/Pt(i);
94  end
95  posisstable;
96
97
98  %The time vector is given here. The first column is zero, the next is
        deltat, the third is 2 times deltat,.. The last column is tmax−
        deltat
99  nsteg=tmax/deltat;
100 t=0:deltat:tmax−deltat;
101
102 %Different matrices are defined here. They first consists of only
        zeroes except the first row which consists of the starting values
        for the different variables.
103 Q1=zeros(5,nsteg);
104 Q1(:,1)= Q0;
105
106 Q2=zeros(5,nsteg);
107 Q2(:,1)= Q0;
108
109 p_acc=zeros(5,nsteg);
110 p_acc(:,1)=P1;
111
112 Hp=zeros(5,nsteg);
113 Hp(:,1)= Hp_Q0;
114
115 %In the beginning the system is a steady state. This means that the
        time derivative is zero. In order to have this it is necessary to
        introduce a term which is due to the difference in initial
```

```matlab
         pressure in accumulator and in the pressure delivered by the pump.
116  diff_pacc_Hp=Hp_Q0−(p_acc(:,1)/(rho∗g));

117
118  %Next the solution process of the differential equations are
         implemented. The outer for loop is counting which frequency is
         studied while the inner  for loop counts which time step are
         ongoing. The if criteria is the small perturbation in volume flow
         which happens when 10% of tmax is calculated. This is done to
         check that the system is at steady state before the perturbation.
         The equations are solved with Euler's method.
119  for  j=1:5
120      for  i=1:nsteg−1
121          if  i==nsteg/10
122              Q2(j,i)=Q2(j,i)∗1.001;
123          end
124          Hp(j,i)=finn_Hp(Q2(j,i), a(j), b(j), c(j),Qstar(j), H0(j));
125          Q2(j,i+1)=Q2(j,i)+deltat∗3600∗g∗A/L2∗(Hp(j)−1/(rho∗g)∗p_acc(j
                ,i)−diff_pacc_Hp(j));
126          p_acc(j,i+1)=p_acc(j,i)+deltat∗(Q2(j,i)−Q1(j,i))/3600∗(p0(j)∗
                kappa/(volumeexp(j)∗A_acc∗L_acc));%+(1/A_acc∗rho∗g));
127          Q1(j,i+1)=Q1(j,i)+deltat∗3600∗g∗A/L1∗(p_acc(j,i)/(rho∗g)−k(j)
                ∗Q1(j,i)^2+diff_pacc_Hp(j)−Hst);
128      end
129  end

130
131  %Figure 3 plots the pressure in the accumulator over time.
132  figure(3)
133  plot(t,p_acc)
134  legend('Surge shaft level, P [Pa]')
135  xlabel('Time [s]')
136  ylabel('Surge shaft level, P [Pa]')

137
138  %The frequency of the mass oscillations are found by looking at the
         period of the oscillations. This is done by taking the difference
         between the highest and the lowest amplitude of the oscillations
         of the pressure in the accumulator. The frequency is then one
         divided by the period.
139  T=zeros(1,5);
140  frek=T;
141  for  i=1:5
142      [imax(i) jmax(i)]=max(Q2(i,:));
143      [imin(i) jmin(i)]=min(Q2(i,:));
144      T(i)=2∗(t(jmax(i))−t(jmin(i)));
145      frek(i)=abs(1/T(i));
146  end

147
148  %The power input, dissipation and power difference is calculated next
         . The power input is given by the pump characteristic while the
         dissipation is given by the system characteristic.
```

```matlab
149  p=zeros(5,length(t));
150  p_in=zeros(5,length(t));
151  p_dis=zeros(5,length(t));
152  for i=1:5
153      for j=1:nsteg-1
154          p_in(i,j)=rho*g*Q2(i,j)*Hp(i,j)/3600;
155          p_dis(i,j)=rho*g/3600*(Hst+k(i)*Q1(i,j)^2)*Q1(i,j);
156          p(i,j)=p_in(i,j)-p_dis(i,j);
157      end
158  end
159
160  %Figure 4 plots the pressure oscillations for the given operational
          point
161  figure(4)
162  plot(t,p)
163  xlabel('Time [s]')
164  ylabel('Power [W]')
165  legend('45 Hz','30 Hz','35 Hz','40 Hz','45 Hz')
166
167  %The mass oscillation frequencies are saved in a matrix called Res
168  Res={'Frequency [Hz]','Helmholtz [Hz]','Mass Oscillations [Hz]';
169      25,helmholtz(1),f_torb(1); ...
170      30,helmholtz(2),f_torb(2);...
171      35,helmholtz(3),f_torb(3);...
172      40,helmholtz(4),f_torb(4);...
173      45,helmholtz(5),f_torb(5)};
174
175  %The Res matrix is here written to Excel.
176  xlswrite('Frekvenskalkulasjon.xlsx',Res,2,'A2:C7')
177
178  %The frequency of the mass oscillations are written to Excel. The
          frequency varies with operational point and with rotational
          frequency.
179  if Q0<50
180      xlswrite('Frekvenskalkulasjon.xlsx',frek',2,'D12:D16')
181  elseif Q0==50
182      xlswrite('Frekvenskalkulasjon.xlsx',frek',2,'D21:D25')
183  elseif Q0==100
184      xlswrite('Frekvenskalkulasjon.xlsx',frek',2,'D31:D35')
185  elseif Q0==150
186      xlswrite('Frekvenskalkulasjon.xlsx',frek',2,'D40:D44')
187  elseif Q0==200
188      xlswrite('Frekvenskalkulasjon.xlsx',frek',2,'D49:D53')
189  elseif Q0==250
190      xlswrite('Frekvenskalkulasjon.xlsx',frek',2,'D58:D62')
191  elseif Q0==300
192      xlswrite('Frekvenskalkulasjon.xlsx',frek',2,'D67:D71')
193  elseif Q0==350
194      xlswrite('Frekvenskalkulasjon.xlsx',frek',2,'D76:D80')
```

```matlab
195  elseif Q0==400
196      xlswrite('Frekvenskalkulasjon.xlsx',frek',2,'D85:D89')
197  elseif Q0==500
198      xlswrite('Frekvenskalkulasjon.xlsx',frek',2,'D94:D98')
199  end
200
201  %The posisstable is also written to Excel
202  if Q0<50
203      xlswrite('Frekvenskalkulasjon.xlsx',posisstable,2,'F12:F16')
204  elseif Q0==50
205      xlswrite('Frekvenskalkulasjon.xlsx',posisstable,2,'F21:F25')
206  elseif Q0==100
207      xlswrite('Frekvenskalkulasjon.xlsx',posisstable,2,'F31:F35')
208  elseif Q0==150
209      xlswrite('Frekvenskalkulasjon.xlsx',posisstable,2,'F40:F44')
210  elseif Q0==200
211      xlswrite('Frekvenskalkulasjon.xlsx',posisstable,2,'F49:F53')
212  elseif Q0==250
213      xlswrite('Frekvenskalkulasjon.xlsx',posisstable,2,'F58:F62')
214  elseif Q0==300
215      xlswrite('Frekvenskalkulasjon.xlsx',posisstable,2,'F67:F71')
216  elseif Q0==350
217      xlswrite('Frekvenskalkulasjon.xlsx',posisstable,2,'F76:F80')
218  elseif Q0==400
219      xlswrite('Frekvenskalkulasjon.xlsx',posisstable,2,'F85:F89')
220  elseif Q0==500
221      xlswrite('Frekvenskalkulasjon.xlsx',posisstable,2,'F94:F98')
222  end
223
224  %At the end of the script the code is transformed to latex.
225  %dyn=publish('Dynamisk.m','latex');
```